DEVELOPMENT OF A DEFENSE METEOROLOGICAL SATELLITE PROGRAM (DMSP) F-15 DISTURBANCE STORM-TIME (Dst) INDEX

THESIS

James M. Bono, Captain, USAF

AFIT/GAP/ENP/05-02

DEPARTMENT OF THE AIR FORCE

AIR UNIVERSITY

AIR FORCE INSTITUTE OF TECHNOLOGY

Wright-Patterson Air Force Base, Ohio

AFIT/GAP/ENP/05-02

DEVELOPMENT OF A DEFENSE METEOROLOGICAL SATELLITE PROGRAM (DMSP) F-15 DISTURBANCE STORM-TIME (Dst) INDEX

THESIS

Presented to the Faculty

Department of Engineering Physics

Graduate School of Engineering and Management

Air Force Institute of Technology

Air University

Air Education and Training Command

In Partial Fulfillment of the Requirements for the

Degree of Master of Science (Applied Physics)

James M. Bono, BS

Captain, USAF

March 2005

AFIT/GAP/ENP/05-02

DEVELOPMENT OF A DEFENSE METEOROLOGICAL SATELLITE PROGRAM (DMSP) F-15 DISTURBANCE STORM-TIME (Dst) INDEX

James M. Bono, BS
Captain, USAF

Approved:

/signed/	28 March 2005
Major Devin Della-Rose (Chairman)	Date
/signed/	28 March 2005
Dr. Fred Rich (Member)	Date
/signed/	28 March 2005
Dr. Dursun Bulutoglu (Member)	Date

Abstract

As the Department of Defense's use of space and space assets increases, so does its need for timely and accurate predictions of space weather conditions. A good understanding of the data from satellites together with data from ground stations can help model and determine variations in the space environment. An accurate, real-time Disturbance storm-time (Dst) index would be a primary input into current and future space weather models.

The Dst index is a measure of geomagnetic activity used to assess the severity of magnetic storms. The index is based on the average value of the horizontal component of the Earth's magnetic field measured at four ground-based observatories. Use of the Dst as an index of storm strength is possible since the strength of the surface magnetic field at low latitudes is proportional to the energy content of the ring current, which increases during magnetic storms. Since ground-based magnetometers are not Air Force owned, development of a Dst index using the magnetometer from a DMSP satellite would remove the Air Force Weather Agency's reliance on outside Dst sources

This research presents a method to create a Dst-like index using the magnetometer of the DMSP F-15 satellite. The solar quiet signal was determined for this magnetometer, and the resulting "Dst" index was compared against the official World Data Center Dst for several magnetic storms. Statistical analysis was accomplished using the paired *t*-test which shows good agreement between the DMSP derived Dst and ground-based index. In all of the storms analyzed, statistical results; mean, standard

deviation, confidence intervals, etc., were always an order of magnitude smaller than the presented factors for error.

Acknowledgments

Professionally, this research, and my entire time here at AFIT, would have proved much more difficult if not for the tireless help and dedicated tutelage of Major Della-Rose. He always spent many hours answering questions during difficult times and one to pat you on the back for your successes. Also, I'd like to thank Dr. Fred Rich for providing the data and subject matter of this research and Dr. Dursun Bulutoglu for his statistical expertise.

Personally, I would like to thank my wife for her love and constant support given to me. She has seen me through all that the Air Force has thrown my way. Having you by my side has helped me to accomplish many personal goals which would not have been as rewarding and enjoyable if not shared with someone special.

Lastly, to my step-daughters, let this work serve as a reminder that anything is possible through hard work and perseverance. No matter how small the endeavor, always do your best.

James M. Bono

Table of Contents

Page

List of Figures

Figure Page

Figure Page

List of Tables

Table Page

DEVELOPMENT OF A DEFENSE METEOROLOGICAL SATELLITE PROGRAM (DMSP) F-15 DISTURBANCE STORM-TIME (Dst) INDEX

I. Introduction

1.1 Problem Statement

The Air Force Weather Agency (AFWA) is responsible for measuring and predicting environmental impacts from the "mud to the sun". While the tropospheric meteorologist is only concerned with the lowest 12 km of the atmosphere, the space weather forecaster has an operational area that extends approximately 150 million km to the Sun. The need to understand and predict how space weather affects Department of Defense (DoD) and USAF assets increases as we continually rely on space-based systems to conduct global communications, navigation, command and control, intelligence collection, and theater defense. Space weather refers to disturbances in the solar-terrestrial environment that can degrade or disrupt military systems that operate in or through space (*Citrone, 2002*). Current military systems potentially impacted by space weather phenomena include satellite communications, high frequency radio communications, Global Positioning System (GPS) receivers, ground-based missile-warning/space surveillance radars, orbiting satellites, and high-altitude aircraft.

As our use of space increases, so does our need for timely and accurate predictions of space weather conditions to protect the nation's investment in these critically important systems. Unlike the weather situation on Earth, where observations

at thousands of locations around the world are recorded, weather conditions in space are monitored by only a handful of space-based and ground-based facilities. Space weather forecasters are required to predict conditions in space using a minimum of guidance from actual measurements. A good understanding of the data from satellites together with data from ground observing stations and other sources can help model and determine variations in the space environment. With reliable forecasts, space weather intelligence can be injected into the decision making process enabling commanders and warfighters to anticipate space weather impacts on friendly and adversary systems and exploit this information to optimize operations and planning.

1.2 The Disturbance Storm-Time (Dst) Index

The Dst or disturbance storm time index is a measure of geomagnetic activity used to assess the severity of magnetic storms. It is expressed in nanoteslas and is based on the average value of deviations in the horizontal component of the Earth's magnetic field measured hourly at four near-equatorial geomagnetic observatories. Use of the Dst as an index of storm strength is possible because the strength of the surface magnetic field at low latitudes is proportional to the energy content of the ring current, which increases during geomagnetic storms (Dst decreases as the ring current is energized). Figure 1.1 depicts the case of a classic magnetic storm, the Dst shows a sudden rise, corresponding to the storm sudden commencement, and then decreases sharply, known as the main-phase, as the ring current intensifies. Once the interplanetary magnetic field (IMF) returns northward, and the ring current begins to recover, the Dst begins a slow rise back to its quiet time level. The relationship of proportionality between the horizontal component of

the magnetic field and the energy content of the ring current is known as the Dessler-Parker-Sckopke relation. My method for obtaining Dst will replace the near-equatorial ground-based observatories with magnetometer readings from the Defense Meteorological Satellite Program (DMSP). I will apply this method to data to the F-15 satellite, but it can be extended to all DMSP spacecraft with a boom-mounted magnetometer.

1.3 How the Air Force Weather Agency (AFWA) uses Dst

Currently, AFWA does not have the capability to produce a forecast or real-time Dst index while AFWA's Space Weather Operations Center does not utilize the Dst index. With the future implimentation of the Magnetospheric Specification and Forecast Model (MSFM) the need exists for the capability of producing a real-time Dst index. A quick-look index is available from the World Data Center for Geomagnetism, Kyoto University, Japan, but AFWA would prefer to calculate its own index value based on DoD-owned data, to ensure continuous warfighter support. MSFM will fulfill an AFWA requirement to host/run an assimilative magnetospheric model which would use both observed and forecasted parameters. The real-time Dst would be a primary input into the MSFM. Having this capability would allow for an easier transition of future models and will be used to help with spacecraft anomaly assessments (*Shauna Kinkela, AFWA, private communication 2004*).

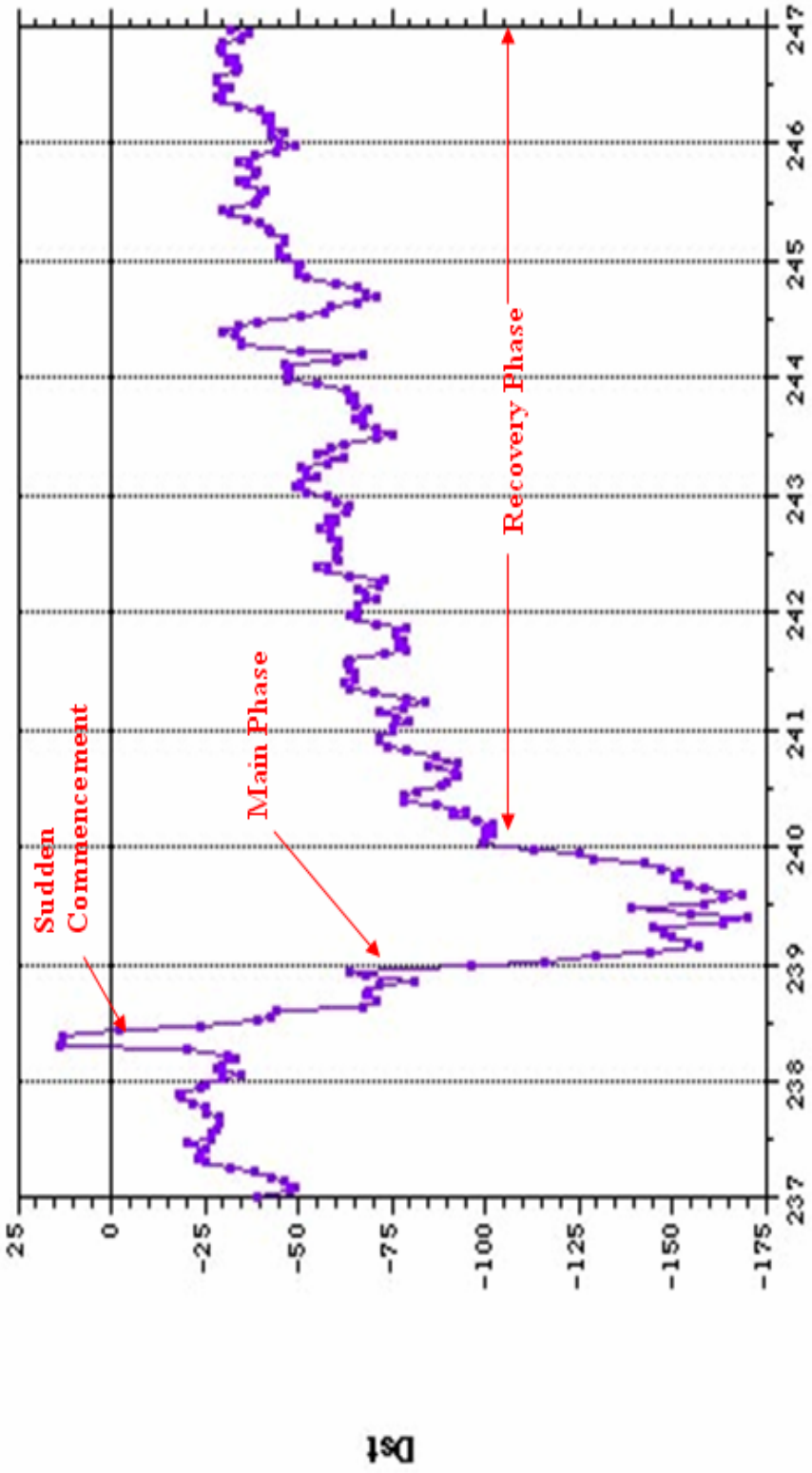

Figure 1.1. Trace of the Dst Index during a magnetic storm.

1.4 The Need for a DMSP Satellite Derived Dst Index

Obtaining magnetometer data from DMSP satellites can be a key factor in developing a usable Dst index for ingesting into MSFM and other space weather models. Use of the DMSP magnetometer data would remove AFWA's reliance on the outside sources for computing the index. Also, satellite magnetometers have the advantage of not having to scale for latitude as is the case for the ground magnetometers.

II. Background

2.1 The Space Environment

The Earth's geomagnetic field produces a semi-permeable obstacle, the magnetosphere, to the solar wind and produces a cavity around which most plasma flows (*Tascione, 1994*). A cross-section of the magnetosphere is shown in Figure 2.1. The ring current can be seen in the middle of the figure. The size of the magnetosphere is determined by the pressure balance. Magnetospheres are very asymmetric. They are compressed on the side facing the solar wind and elongated in the other direction, forming a magnetic tail. The sunward magnetopause on the equator for the Earth is located typically at about 10 earth radii (Re) (*Parks, 2004*). The near-Earth environment consists of a neutral and ionized atmosphere. The magnetosphere, within the Earth's ionized atmosphere, is also composed of the ionosphere (70 km to 1000 km) and plasmasphere (1000 km to 4 Earth radii (Re)) as measured on the equator. Just beyond the near-Earth environment is interplanetary space which is dominated by a high speed, tenuous plasma streaming out from the Sun's corona. This plasma, an ionized gas flowing out into interplanetary space, is known as the solar wind (*Rich, 1994*).

2.1.1 The Solar Cycle

The solar cycle is a measure of the periodic variation of the level of activity on the Sun. The most obvious feature which changes are the number of sunspots visible on the surface of the Sun. The number of sunspots on the Sun is not constant. In addition to the obvious variation caused by the Sun's rotation (sunspots disappear from view and then re-

appear), over time new sunspot groups form and old ones decay and fade away. When viewed over short periods of time (a few weeks or months), this variation in the number of sunspots might seem to be random. However, observations over many years reveal a remarkable feature of the Sun: the number of sunspots varies in a periodic manner, usually described as the 11 year cycle (in actuality, the period varies, and has been closer to 10.5 years this century). The 11 year sunspot cycle is related to a 22 year cycle for the reversal of the Sun's magnetic field. In 1848 Johann Rudolf Wolf devised a method of counting sunspots on the solar disk called the Wolf number. Today the Wolf number (averaged from many observing sites) is used to keep track of the solar cycle. Although the number of sunspots is the most easily observed feature, essentially all aspects of the Sun and solar activity are influenced by the solar cycle. Because solar activity, such as a magnetic storm, is more frequent at solar maximum and less frequent at solar minimum, geomagnetic activity also follows the solar cycle (*Hathaway, 2004*).

The level of the geomagnetic activity is measured using different activity indices, most of which are based on ground-based magnetometer recordings. These recordings can be used to study the longer trends in the solar activity. Variability in the geomagnetic activity has several sources. These sources are; variability in the Sun itself that is reflected in the solar wind, the 11 and 22-year solar cycles, the 1.3 year variability (which involves the Earth's orbit around the Sun taking it to different solar latitudes (annual variability)) (*Zieger and Mursula, 1998)*, the Earth's orbit around the Sun that changes the orientation of relevant coordinate systems (semi-annual variation) (*Russel and McPherron, 1973*), rotation of the Sun around its axis, which can lead to periodicities at

27 days and 13-14 days known as recurrent variability. Figure 2.2 shows the periodic nature of the solar cycle throughout the last two and a half centuries.

2.1.2 The Ring Current

The ring current is one of the major current systems in the Earth's magnetosphere. It circles the Earth in the equatorial plane and is generated by the longitudinal drift of energetic (10 to 200 keV) charged particles. Figure 2.3 shows the ring current. The charged particles that make up the ring current and radiation belts are trapped in the Earth's magnetic field, bouncing back and forth along the magnetic field lines between "mirror points" in the northern and southern hemispheres (*Hamilton, 1988*). These are the points in a non-uniform magnetic field toward either end of a field line where the magnetic field becomes strong enough to cause a particle traveling along that field line to reverse direction. In addition to their bounce motion, the trapped particles also drift azimuthally (in longitude): ions to the west, electrons to the east. It is this drift motion that creates the ring current. The two-dimensional surface that these particles define through their combined bounce and drift motions is known as a "drift shell" or "L shell". Locations within the ring current/radiation belt region of the inner magnetosphere are typically given in terms of the distance, in Earth radii, from the center of the Earth to the point where a particular drift or L shell intersects the plane of the geomagnetic equator.

Charged particles that make up the ring current are trapped on field lines between L~2 and 7. During geomagnetic storms, ring current particle fluxes are dramatically increased, with the peak enhancements occurring in the inner portion (at $L < 4$). The quiet-time ring current consists predominantly of the hydrogen ion, H^+, while the storm-

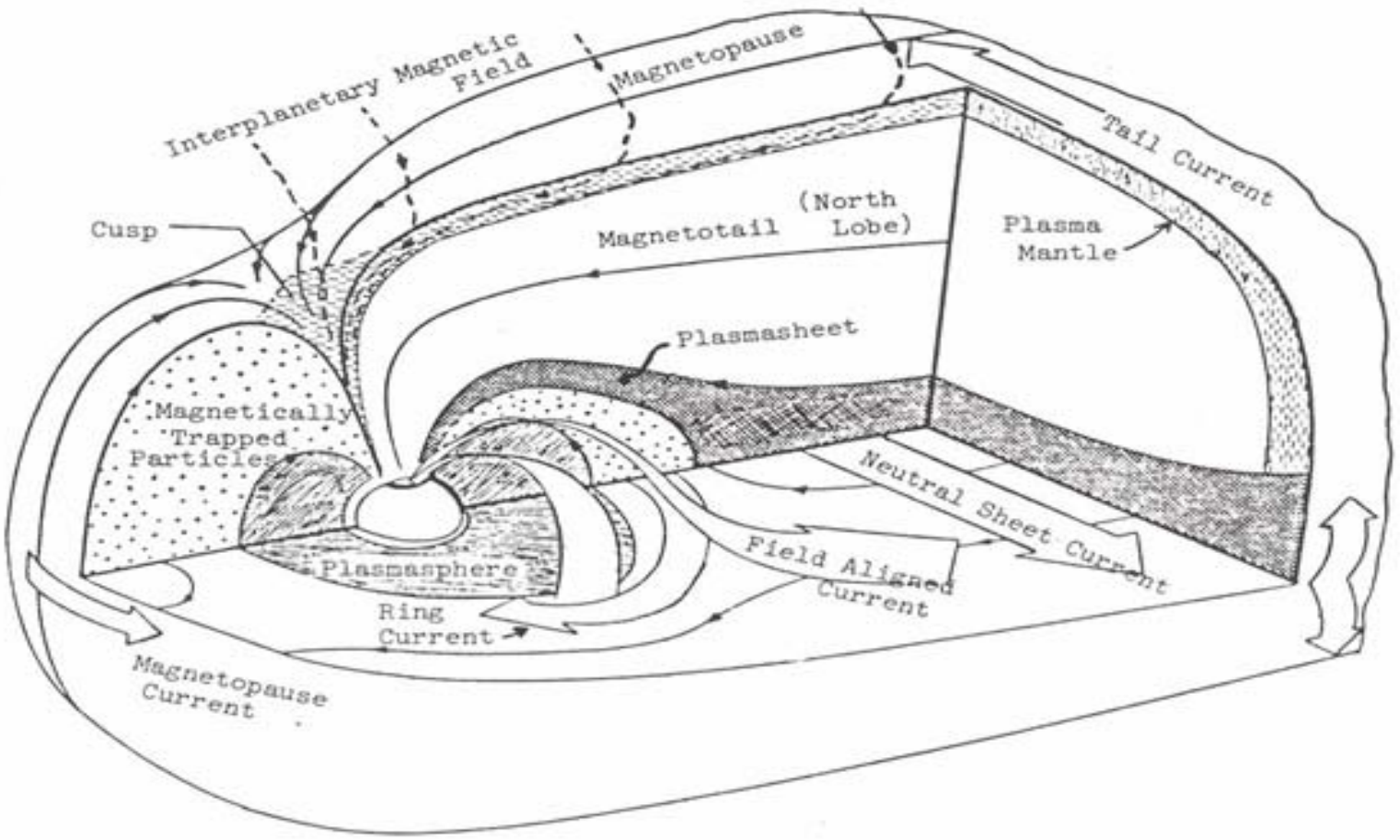

Figure 2.1. A cross-section of the magnetosphere (Tascione, 1994).

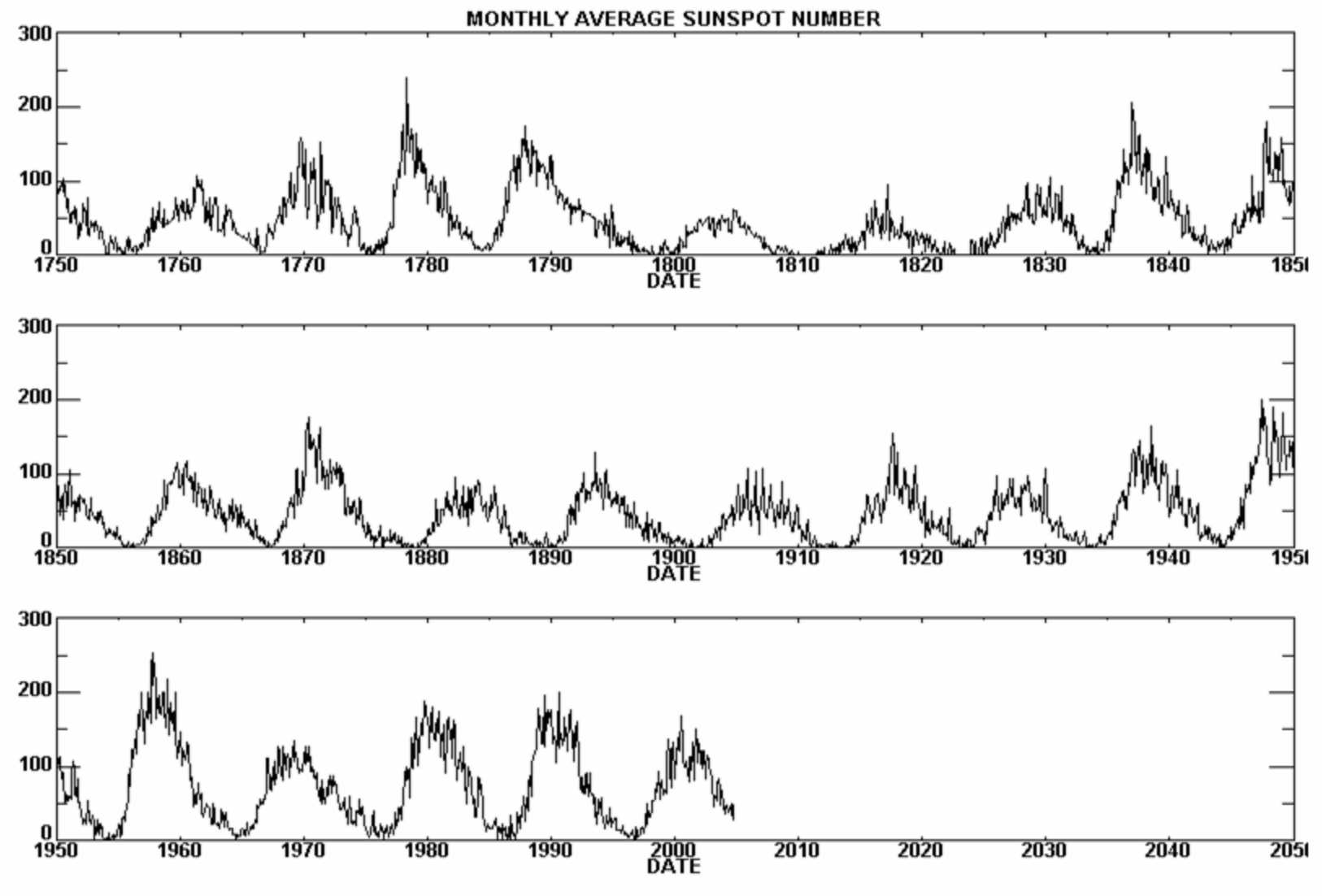

Figure 2.2. The solar cycle. (http://science.nasa.gov/ssl/pad/solar/images/zurich.gif)

time ring current also contains a significant component of the ionospheric oxygen ion, O+, whose contribution to ring current energy density may even exceed that of H+ for brief periods near the maximum of particularly intense storms.

The formation of the storm-time ring current has been attributed to two different processes: (1) the injection of plasma into the inner magnetosphere during the expansion phase of magnetospheric substorms and (2) increased convective transport of charged particles from the nightside plasma sheet deep ($L < 4$) into the inner magnetosphere as a result of an intensification of the Earth's dawn-dusk convection electric field during extended periods of a strong southward Interplanetary Magnetic Field (IMF). The present understanding of ring current formation tends to favor the enhanced convection model over the substorm plasma injection model; however, it is recognized that substorms, while not the primary driver, nonetheless play a significant role in the growth of the storm-time ring current (e. g., by energizing ions in the near-Earth plasma sheet prior to their transport into the ring current) (*Hamilton, 1988*).

The storm-time growth of the ring current lasts from 3 to 12 hours and constitutes the "main phase" of a magnetic storm. Following this main phase, the ring current begins to decay, returning to its pre-storm state in two to three days. (Full recovery can require as long as a month in the case of major geomagnetic storms). During the storm recovery phase, particle transport into the ring current slows, allowing various loss processes to reduce ring current particle fluxes to their quiet-time level.

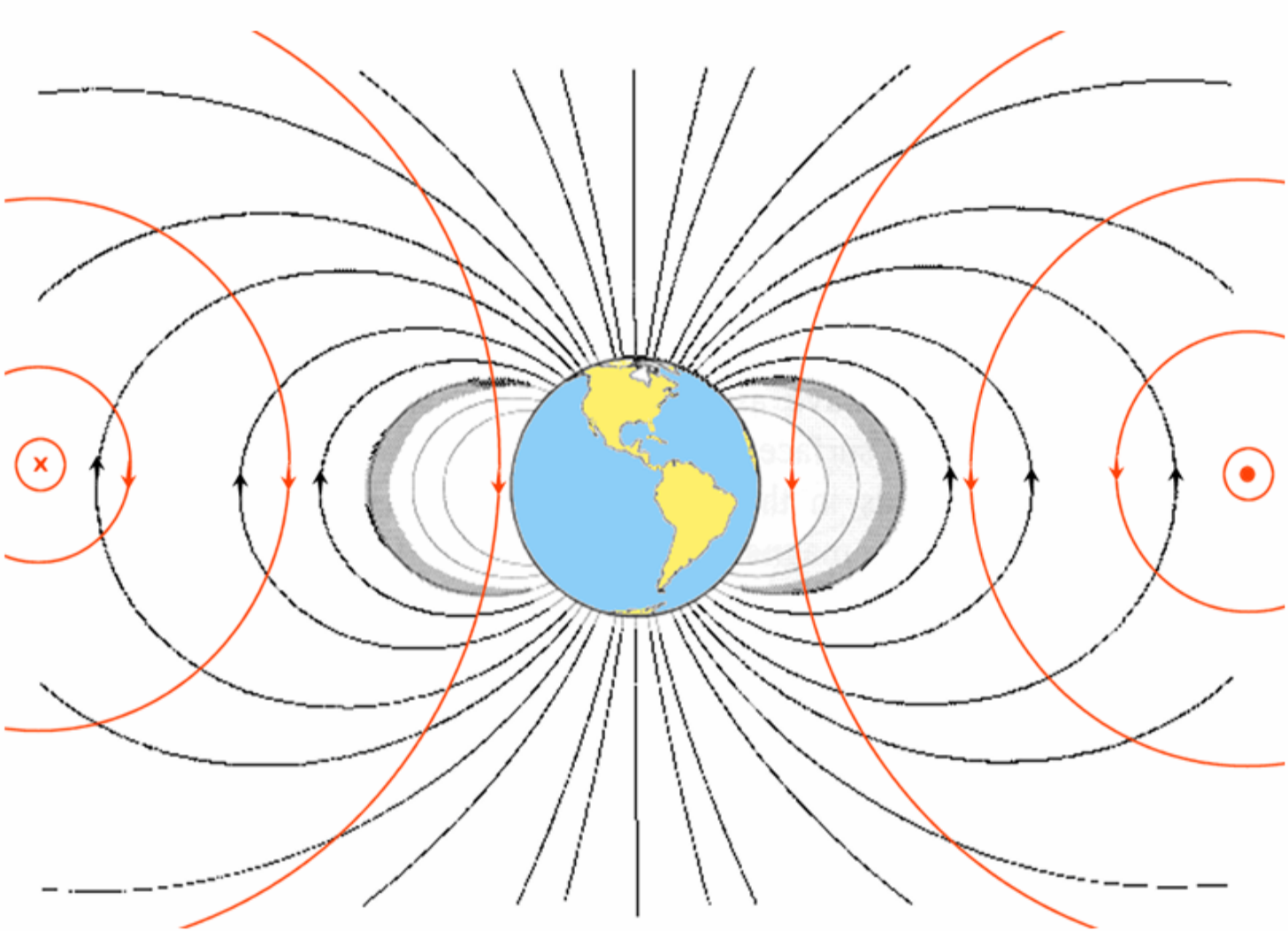

Figure 2.3. The orange rings show the ring current. The X corresponds to current into the page while bold dot refers to current out of the page. The black lines are magnetic field lines. (Rich, Phillips Laboratory 2004)

2.1.3 Solar Quiet (Sq) Signal

When applied to the geomagnetic field, solar quiet is a descriptive word specifically meaning geomagnetic levels such that the Ap geomagnetic index is less than 8. More generally, solar quiet refers to a period of time when the space environment is storm-free. Various "solar quiet" current systems, such as the ionospheric dynamo current, still flow during calm periods. Thus, the first step in investigating magnetic storms is to model this "solar quiet" signal, so it may be removed from magnetic measurements taken during space weather storms.

2.1.3.1 Solar Quiet Current System

As the name implies, the Sq current system is driven by the sun and its characteristics are defined during geomagnetically quiet periods. The process responsible for Sq currents is the thermospheric (neutral) winds that push the conducting ionosphere across the Earth's magnetic field. This produces an electromotive force via Faraday's Law, and the result is the current system illustrated in Figure 2.4. The figure shows the Sq system during equinox. On the dayside, differential solar heating produces high pressure at low latitudes. Thermospheric winds in both hemispheres blow generally poleward in response to the resulting pressure gradient. This sets up a two-cell Sq current system in the dayside *E*-region. At night the winds blow equatorward, reversing the current flow directions in the nighttime cells. However, current magnitudes are much smaller because nighttime ionospheric densities are reduced by one to two orders of magnitude. This entire pattern is fixed to the sun and the Earth rotates underneath it. (*Della-Rose,* 1999)

The nature of the Sq current system has a marked effect on determining a satellite based Dst index. As will be outlined in my Methodology section, an ascending and descending solar quiet value will need to be calculated due to the Sq current system being stronger during the day than at night. The separate calculations are required since the orbit of the F-15 satellite (see section 2.5.1) makes its ascending pass during darkness and its descending pass during the day.

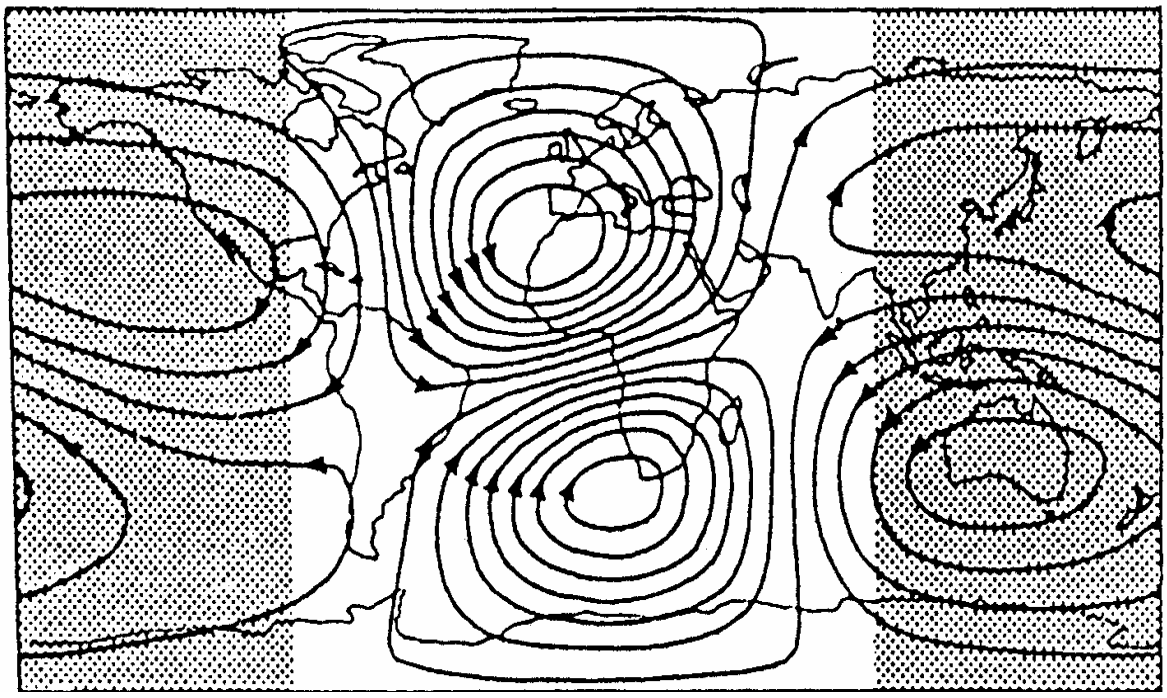

Figure 2.4. The solar quiet current system during equinox. (Volland, 1884)

2.2 Geomagnetic Indices

In an effort to estimate the level of geomagnetic activity, scientists have developed a series of indices designed to give a semi-quantitative measure of this activity. Also, most solar-terrestrial models need geomagnetic indices to specify the solar and magnetic disturbance level. These indices are usually parameters that can be monitored continuously with ground-based equipment or that can be derived from continuously monitored parameters. The reason for the popularity of magnetic indices is twofold. First, they allow researchers to condense vast amounts of data into manageable parameters which are presumably correlated with space weather storming. Second, the correlations established between indices and other space physics parameters can help scientists further unlock the physics of space weather storms.

The four most commonly used indices are Kp, ap, AE, and Dst. The Kp index is a 3-hour index on a quasi-logarithmic scale of the level of worldwide geomagnetic activity. The index is derived from a statistical composite of variations from a selected group of sub-auroral zone stations. The 3-hourly ap index is a linear scaled index obtained directly from Kp. The AE index describes the disturbance level recorded by auroral zone magnetometers. Again, the Dst index monitors the global variations of the ring current, which encircles the Earth close to the magnetic equator in the Van Allen belt of the magnetosphere and will be the focus of my research (*Rostoker, 1972*).

2.3 Ground-Based Magnetometers

AFWA maintains ground-based magnetometer stations to observe the ionosphere-magnetosphere environment. In addition, AFWA receives space environmental data

from the National Oceanographic and Atmospheric Administration (NOAA) operated ground-based observatories, and stations operated by other agencies and countries. The basic sensor package at most observatories consist of a triaxial fluxgate magnetometer which gathers 3-D magnetic data, typically the horizontal intensity, declination, and the vertical component (H, D, and Z respectively), plus a proton magnetometer, which measures the total intensity of the field (F). The redundancy between these two measurement systems allows for consistency checks that are useful for troubleshooting. Moreover, a flux-gate sensor-electronics package is prone to deliver data that drift on an absolute scale, primarily as the result of changes in ambient temperature; proton magnetometer data also drift with temperature, but usually much less than flux-gate data. To reduce this baseline drift, the sensors and electronics are housed in well-insulated, thermostatically-controlled buildings. Observatory standards must be consistent with those set by Intermagnet, an international consortium which promotes the worldwide collection of high-quality, ground-based magnetometer data.

2.4 Ground-Based Dst Index

Discussion of an index to monitor the equatorial ring current variation were started in the late 1940's by J. Bartels, chairman of the Committee on Characterization of Magnetic Disturbances of the International Association for Terrestrial Magnetism and Electricity (IATME) which later became the International Association of Geomagnetism and Aeronomy (IAGA). The first attempts at finding a Dst index were made in the late fifties and early sixties. In 1964 M. Suguira published a paper of Dst values and in 1967, Sugiura and Hendricks proposed the first derivation of a Dst index. Due to modifications

in the station network and improvements to the derivation process today's accepted Dst was developed in 1981 by Sugiura. This method forms the basis of the Dst index that I will later compare my DMSP-derived Dst index against. Plots and data using this ground-based method can be found at the Data Analysis Center for Geomagnetism and Space Magnetism Graduate School of Science, Kyoto University, Kyoto, JAPAN via http://swdcwww.kugi.kyoto-u.ac.jp/.

2.4.1 Method for Deriving the Ground-Based Dst Index

Data from a network of four near-equatorial geomagnetic observatories are used to derive Dst. Figure 2.5 is a map of the observatories and gives a table of the geographical coordinates of each. The observatories are located at Honolulu, Hawaii, San Juan, Puerto Rico, Hermanus, South Africa and, Kakioka, Japan. These stations were chosen based on the quality of their observations and because their locations are sufficiently distant from the auroral and equatorial electrojets. The observatories are spatially distributed as evenly as possible. To compute Dst, one must eliminate the magnetic signatures of both the solar quiet currents and the Earth's main (internal) magnetic field (or baseline). These topics are treated in the following two sections.

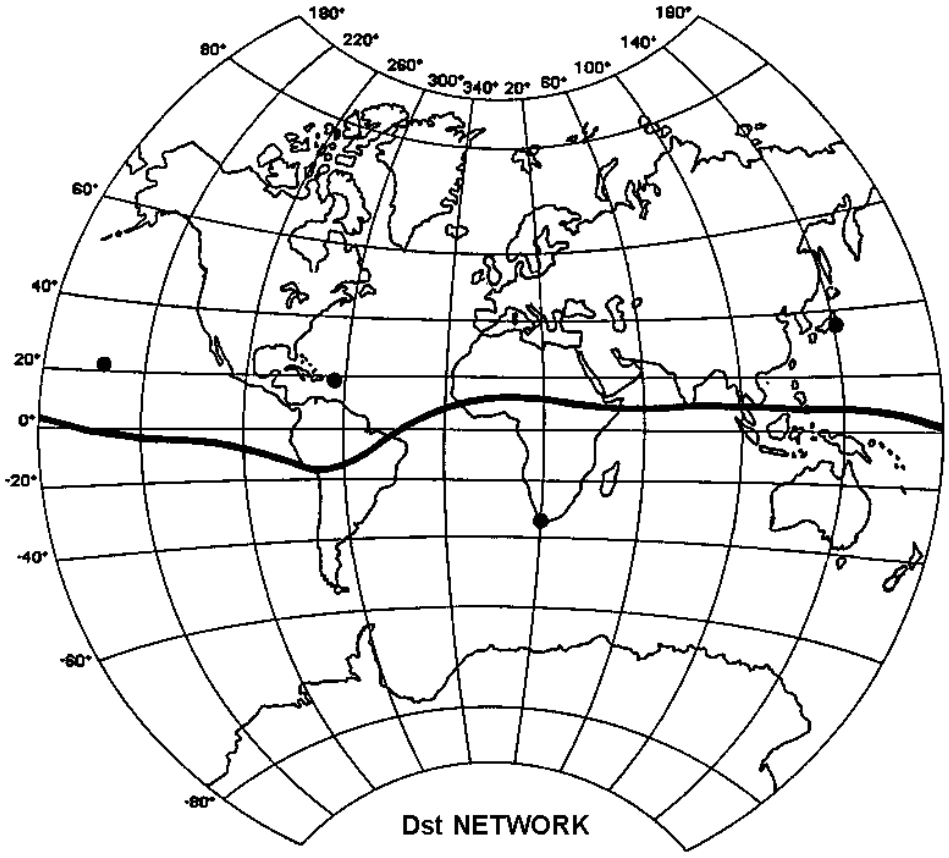

Observatory		Geographic		Geomagnetic
		Longitude (E)	Latitude	Dipole latitude
Hermanus		19.22°	-34.40°	-33.3°
Kakioka		140.18°	36.23°	26.0°
Honolulu	to April 1960	201.90°	21.30°	21.0°
	after April 1960	201.98°	21.32°	21.1°
San Juan	to January 1965	293.88°	18.38°	29.9°

Figure 2.5. Location and coordinates of the magnetic observatories used in the derivation of Dst. (Suguira 1981)

2.4.1.1 Finding the Baseline

The Earth's main field magnetic signature, or baseline, for the horizontal component of the geomagnetic field, H, must be defined for each observatory before Dst can be computed. This baseline changes slowly with time as the Earth's magnetic dynamo changes; this is known as the "secular variation." For each station, the annual mean values of H, calculated from the "five quietest days" (the five quietest days of each particular station not to be confused with the worldwide five international quiet days based on Kp index) of each month form the database for the baseline. The baseline is expressed in a power series in time and the coefficients for terms up to the quadratic are determined by the methods of least squares, using the annual means for the current year and the four preceding years.

The baseline is expressed as

$$H_{base}(\tau) = A + B\,\tau + C\,\tau^2 \qquad (2\text{-}1)$$

Where τ is the time in years measured from the reference epoch.

The baseline value $H_{base}(T)$ calculated from (2-1) for each Universal Time (UT) hour of the current year is subtracted from the observed hourly average H value, $H_{obs}(T)$, to form the hourly average station deviation, $\Delta H(T)$:

$$\Delta H(T) = H_{obs}(T) - H_{base}(T) \qquad (2\text{-}2)$$

These hourly station deviations, combined with a knowledge of the station solar quiet (Sq) magnetic signatures (described below), form the basis of the Dst index computation.

2.4.1.2 Solar Quiet Signal (Sq) Determination

The average solar quiet variation, Sq, for each month is determined from the values of H(t) for the internationally selected five quietest days of the month (as stated, these days are determined by having the lowest Kp value of all the days of that particular month). The quietest days are determined as a function of UT time. To define an average Sq variation for the local day of each observatory, averages are formed for the local hours using five local days that have the maximum overlap with the international five quietest days. Using the hourly values immediately before and after the selected local days, the linear change is found and subtracted from the Sq variation. This method removes the non-cyclic change, which is part of the Dst variation. The 12 sets of the monthly average Sq determined for the year are expanded in a double Fourier series with the local time, t, and the month number, s, as follows:

$$Sq(t,s) = \sum\sum A_{mn}\cos(mt + \alpha_m)\cos(ns + \beta_n) \qquad (2\text{-}3)$$

This equation allows for calculation of Sq(T) at any UT hour, T, of the year. This procedure is applied to each of the four observatories.

2.4.1.3 Hourly Equatorial Dst Index

For each observatory the hourly disturbance variation, D(T), is given by:

$$D(T) = \Delta H(T) - Sq(T) \qquad (2\text{-}4)$$

D(T) is then averaged over the four observatories and normalized to the dipole equator by:

$$Dst(T) = D(T)/\cos\varphi \qquad (2\text{-}5)$$

Where the denominator is the average of the cosines of the dipole latitudes, φ_i (I = 1,4), of the observatories contributing to the average. The normalization procedure minimizes the undesired effects from missing hourly values. Figure 2.6 shows a Dst plot for November 2001 from the Kyoto website (*Entire section from Sugiura and Toyohisa, 1986*).

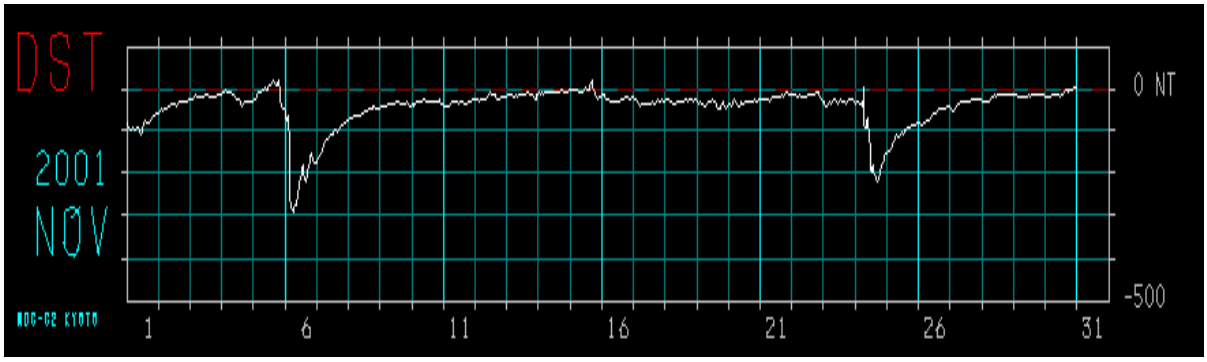

Figure 2.6. A plot of Dst for the month of November 2001. (Kyoto University website)

2.5 The DMSP Satellite

The Defense Meteorological Satellite Program (DMSP) is a Department of Defense (DoD) program run by the Air Force Space and Missile Systems Center (SMC). The DMSP designs, builds, launches, and maintains satellites monitoring the meteorological, oceanographic, and solar-terrestrial environments. The DMSP mission is to provide global visible and infrared cloud data and other specialized meteorological, oceanographic and solar-geophysical data in support of DoD operations. The first DMSP spacecraft was launched in January 1965 and the latest (F-16) was launched in late 2003. The satellites are in near circular, sun-synchronous, polar orbits at an altitude between 835 to 850 km. AFWA uses data from DMSP satellites for determining, on an hourly basis, the state of both the tropospheric and the space environments (*Rich, 1994*). F-15, launched in December of 1999 and still operational, is the satellite whose magnetometer data I used for this research.

2.5.1 The DMSP F-15 Satellite Orbit

As stated, the data for my research comes exclusively from the F-15 satellite particularly the magnetometer data from January 2000 through December 2003. All DMSP satellites are polar-orbiting. The F-15 satellite takes approximately 100 minutes to orbit the globe giving up to 14 orbits per day. Figure 2.7 shows the ascending F-15 satellite. Notice that when the satellite is ascending, going from the southern to northern hemisphere, the orbit is in the nighttime phase. Conversely, Figure 2.8 shows the F-15 in the descending portion of its orbit, traveling from the northern to southern hemisphere, with its orbit in the daytime phase. Also, the figures show the F-15 position at the

magnetic equator. As will be described in the Methodology chapter, the DMSP magnetometer readings at the magnetic equator crossings will be used to determine the Sq signal and the Dst index.

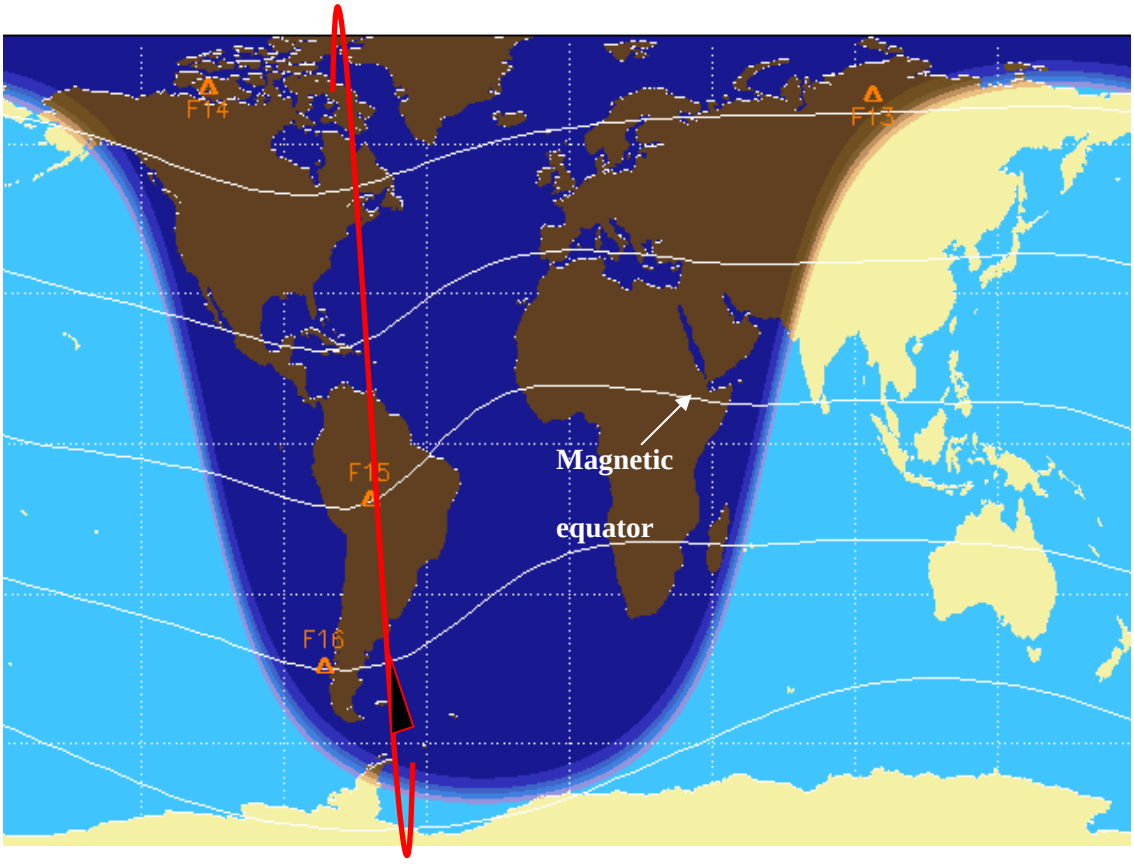

Figure 2.7. DMSP F-15 ascending, nighttime phase orbit. (https://swx.plh.af.mil/dmsp.html)

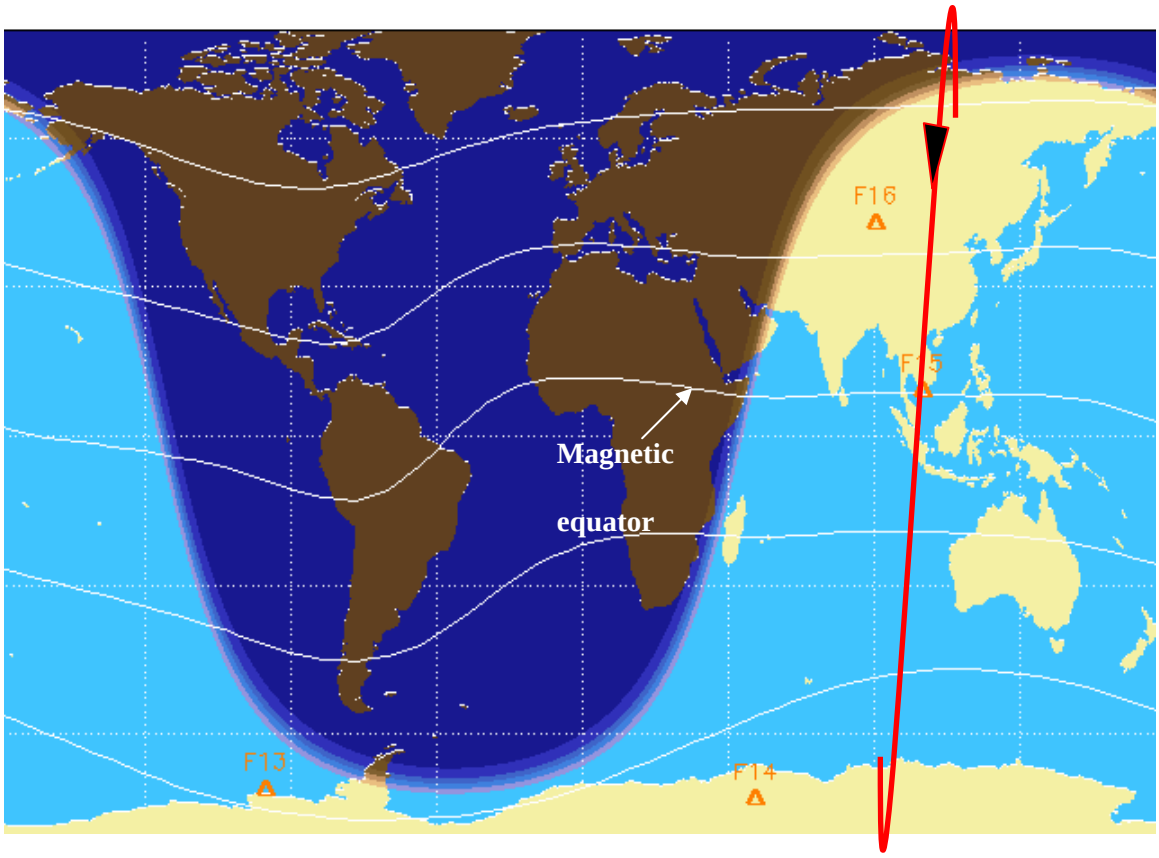

Figure 2.8. DMSP F-15 descending, daytime phase orbit. (https://swx.plh.af.mil/dmsp.html)

2.6 Special Sensor Magnetometer (SSM) and Coordinate System

DMSP spacecraft are outfitted with an array of sophisticated space environmental sensors. The SSM is a triaxial fluxgate magnetometer used as a space environmental sensor for spacecrafts F12 through F20. The instrument was designed and built at NASA's Goddard Spaceflight Center. A "proof of concept" SSM instrument was built from surplus magnetometers by Johns Hopkins University/Applied Physics Laboratory and flown on F7.

The magnetometer measures the strength and direction of the total geomagnetic field at the satellite's location with a range of +/- 64,000 nT with a sensitivity of approximately 50 nT. The magnetic field has three sources: (1) the magnetic field from the solid earth, (2) the magnetic field from electrical currents flowing in the ionosphere and magnetosphere, and (3) the magnetic field from the spacecraft. Measurement of (2) is the main objective of the SSM with (1) being a secondary objective. Source (3), spacecraft noise, is a nuisance and eliminated from the data as much as possible. Since spacecraft noise rapidly decreases in magnitude with increasing distance from the source, the SSM sensor is placed at the end of a 5m boom for spacecrafts F15 to F20. A schematic of spacecraft F15 is shown in Figure 2.9.

The parameters measured by the SSM are the three components of the magnetic field vector. The magnetometer takes and reports 12 readings per second for the Y and Z axes. Only 10 of the 12 readings are reported for the X axis due to telemetry limitations. The SSM's axes are aligned such that X is downward and aligned to local vertical

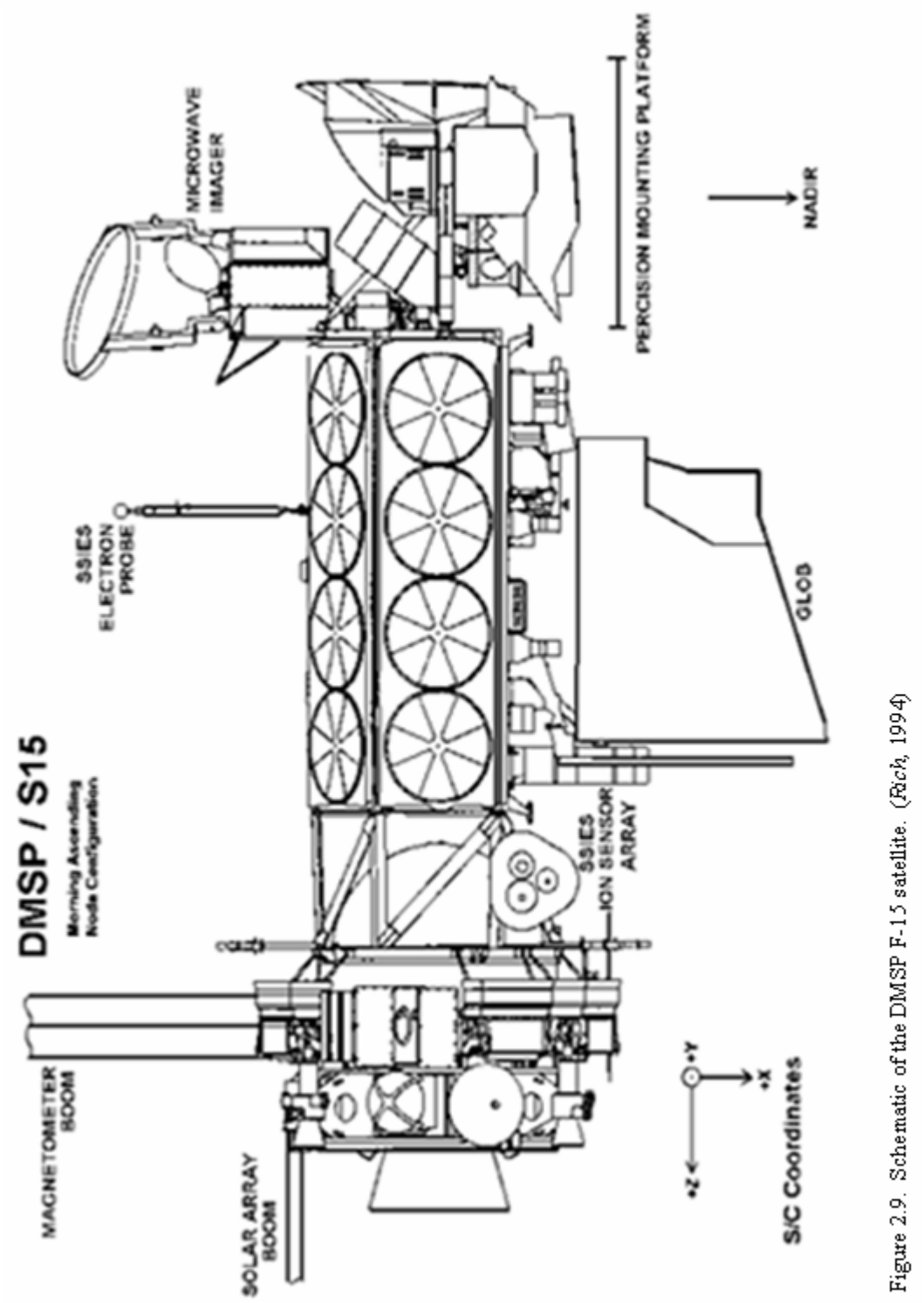

Figure 2.9. Schematic of the DMSP F-15 satellite. (*Rich*, 1994)

within 0.01 degree, Y is parallel to the spacecraft's velocity vector with ascending node in the afternoon/evening sector, and Z is away from the solar panel and anti-parallel to the orbit normal vector. The fluxgate sensors are constructed using a ring core geometry. Figure 2.10 shows a photo of the SSM and the construction of one of three identical sensors. Keys to the design of the sensor are the feedback coil and the sensor core. These elements can be shown to be the most significant sources of error, both in the form of alignment and temperature stability (*Rich, 1994*).

Monitoring of the ionosphere is the primary space environmental mission of the Air Force. Subtracting of the Earth's internal magnetic field from SSM data one can obtain a measurement of the disturbed magnetic field created by electrical currents flowing along geomagnetic field lines from the ionosphere to the magnetosphere. These currents, FACs, are generally confined to the auroral zones (*Rich, 1994*). (All material in this section regarding the SSM instrument was taken from the AFRL Space Weather Center of Excellence, Space Weather Data Survey, website (https://swx.plh.af.mil/).)

2.7 Satellite and SSM Factors for Error and Space Environment Considerations

As with any instrumentation, factors for error must be considered when analyzing the results of the magnetometer readings from the DMSP F-15 satellite. The placement of the SSM on a 5 meter boom started with the F-15 satellite vastly improving magnetometer readings by removing spacecraft noise of body-mounted magnetometers of earlier missions. Even with this improvement many sources for error still exist for the There are four instrument factors for error and two space environments factors that lead to differences between the official Dst index and a satellite-derived index. The

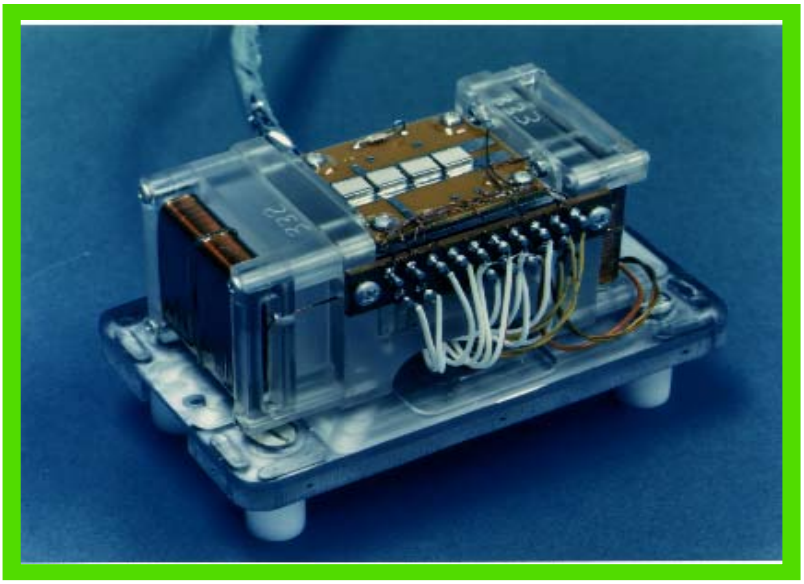

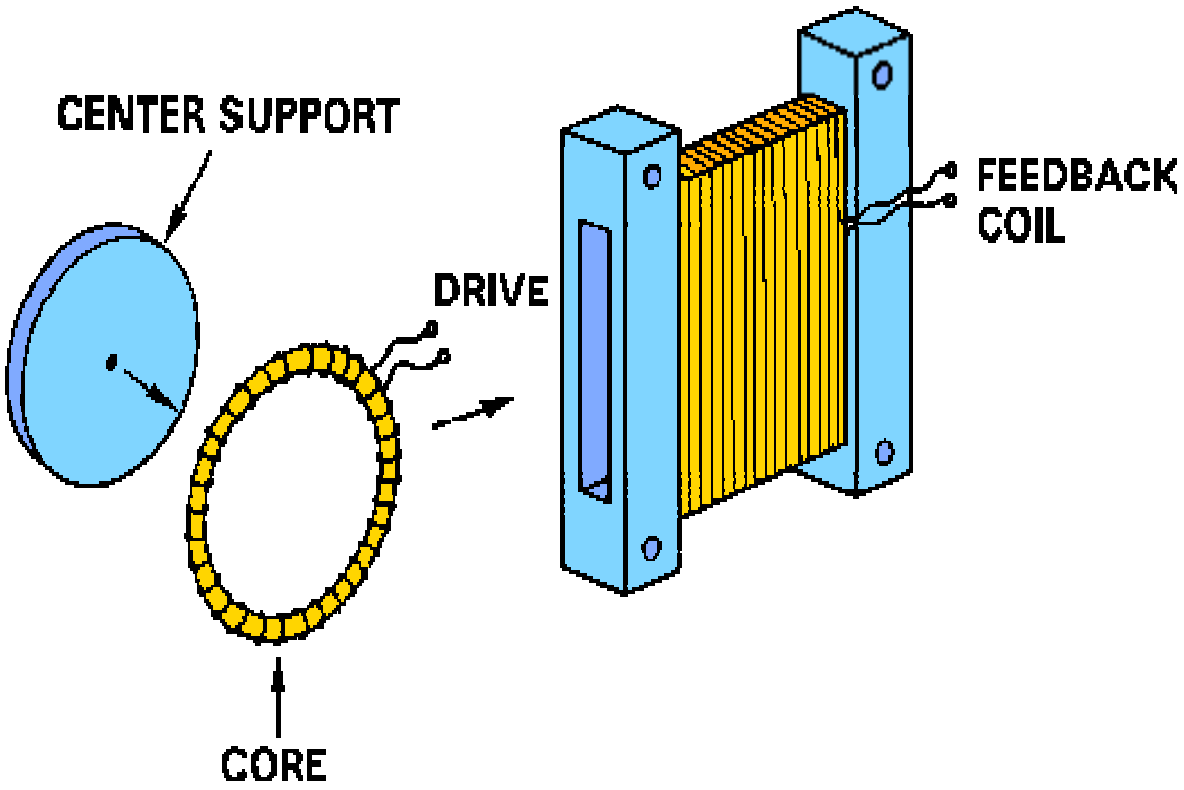

Figure 2.10. Photo and elements of the SSM. (Deloney 2000, Rich, 1998)

SSM errors include calibration errors, the spacecraft's direct current magnetic field, the solar cell magnetic field, and the satellites attitude. The space environment imposes two important factors which are uncertainty in the subtraction of the Earth's main magnetic field and difference between SSM and ground-based magnetometer readings due to the SSM, orbiting at an altitude of approximately 850 km, being closer to the ring current.

As stated the instrument uncertainty value is due to four different factors. First, SSM calibration is documented to be less than 20 nanoteslas (nT) but may be significantly less. Next, the spacecraft's d/c magnetic field at the location of the sensor has been determined to an accuracy of ±20 nT at the time of in-flight calibration. Also, there are orbit dependent variations in the magnetic field that show up in the readings. The solar panel of the satellite rotates 360 degrees per orbit. When the solar panel is closest to the magnetometer the magnetic field related to currents in the panel can be detected with a strength of 5-30 nT. Finally, the spacecraft's attitude is maintained to an accuracy of ±0.010 degrees (most of the time) to ±0.020 degrees (at all times). Since the Earth's field is approximately 45,000 nT over the poles, the lack of alignment knowledge gives an error of up to ±80 nT in the magnetic vector (Bx, By, and Bz).

The local space environment at satellite altitude leads to two significant factors for difference due to the dynamo magnetic field. The International Geomagnetic Reference Field (IGRF) is a mathematical description of the Earth's main magnetic field used widely in studies of the Earth's deep interior, the crust and the ionosphere and magnetosphere. The difference between the IGRF model field and the actual magnetic field at DMSP orbit is approximately ±50 nT over most continental areas. Over poorly

surveyed regions of the globe, this error can be as high as ±150 nT. Lastly, with the satellite location 850 kilometers closer to the ring current than ground-based observatories, one would expect a higher DMSP derived Dst value. (*All factors for error from Rich correspondence, 2004*).

What do all these uncertainties add up to? The short answer turns out to be, "It depends". If all the factors for error acted in concert and operated in the same direction they would add-up to the same magnitude of a sizable magnetic storm (a few hundred nTs). More realistically, some of the error factors will not act in the same direction essentially canceling-out portions of the error.

III. Methodology

3.1 DMSP Derived Dst Index

This section describes the method I used to create my DMSP derived Dst index. The technique is similar to the accepted ground-based method in a couple of ways. First, I obtain the five international quiet days, based on Kp, for each month to obtain a solar quiet signal value for the month with a slight variation that will be described in section 3.3. My method creates an ascending and descending solar quiet signal for each month of each year. My research analyzed four years (2000-2003) of SSM data therefore, each month's solar quiet values were then averaged over the four years to produce a total of two (one ascending and one descending) final Sq values for each month of the year.

Analyzing the Dst for a day with a magnetic storm was accomplished by subtracting the solar quiet value from the magnetometer readings from the satellite. I then averaged the ascending and descending values (after subtraction of Sq signal) and corresponding time of magnetic equator crossing. These results were then plotted with the actual Dst index for the same time period.

3.2 Information and Support from Air Force Research Laboratory (AFRL)

All of the F-15 magnetometer data was provided by Dr. Frederick Rich from AFRL, Space Vehicles Directorate, Hanscom AFB, MA. Dr. Rich provided me with six CDs consisting of SSM data from the F-14 (01 Jan 2000-01 May 2001), F-15 (01 Dec 1999-15 Jul 2004), and F-16 (01 Oct 2003-15 Jul 2004) satellites.

3.2.1 Data Files and the Interactive Data Language (IDL) Program

The CDs contain daily files for the dates listed above. To read the data the files must be read into IDL using a rdssm.pro program which was also provided by Dr. Rich. The program creates a text file tabulating the data as shown in Table 3.1. The table produced lists the year, day (Julian date), hour, minute, and second in UT the magnetometer reading was taken. Also, for each reading, the geomagnetic latitude and longitude and altitude are given. The table also lists the magnetometer reading in seconds for each component of the magnetic field (Delta Bx, Delta By, and Delta Bz). The delta prefix is a result of IDL subtracting the Earth's main field via the IGRF model.

There is an option in the IDL program to create a graphical output. Figure 3.1 show a plot of SSM data for the Bx, By, and Bz components with time shown along the horizontal axis. This particular plot was generated while the satellite ascended from 40 degrees north geographic latitude, traversed the pole, then descended to, again 40°N. Note the peaks in the Bz component. These are due to the field aligned or Birkeland currents located in the higher latitudes, near auroral zones. Although it does not appreciably contribute to the overall geomagnetic configuration, the high-latitude field-aligned current system provides an important coupling mechanism between the magnetosphere and the ionosphere.

3.3 Identifying the Solar Quiet Signal

The current method of finding Dst using ground-based magnetometers is not without complications. As stated previously, the magnetometer stations are evenly distributed near the magnetic equator. The data must then be corrected for the distance

Yr	DAY	HH	MM	SEC	GLAT	GLNG	ALT
2003	324	1	36	2.00	-13.7	298.2	852.1
2003	324	1	37	2.00	-10.2	297.4	851.4
2003	324	1	38	2.00	-6.7	296.6	850.7
2003	324	1	39	2.00	-3.2	295.8	850.2
2003	324	1	40	2.00	0.3	295.0	849.6
2003	324	1	41	2.00	3.9	294.2	849.2
2003	324	1	42	2.00	7.4	293.4	849.0
2003	324	1	43	2.00	10.9	292.6	848.8

Time(sec UT)	Delta-Bx	Delta-By	Delta-Bz
3.5	12.	-61.	9.
4.5	13.	-59.	9.
5.5	13.	-61.	8.
6.5	12.	-60.	9.
7.5	13.	-61.	9.
8.5	14.	-61.	8.
9.5	14.	-60.	8.
10.5	14.	-62.	9.

Table 3.1. IDL text file output of SSM data

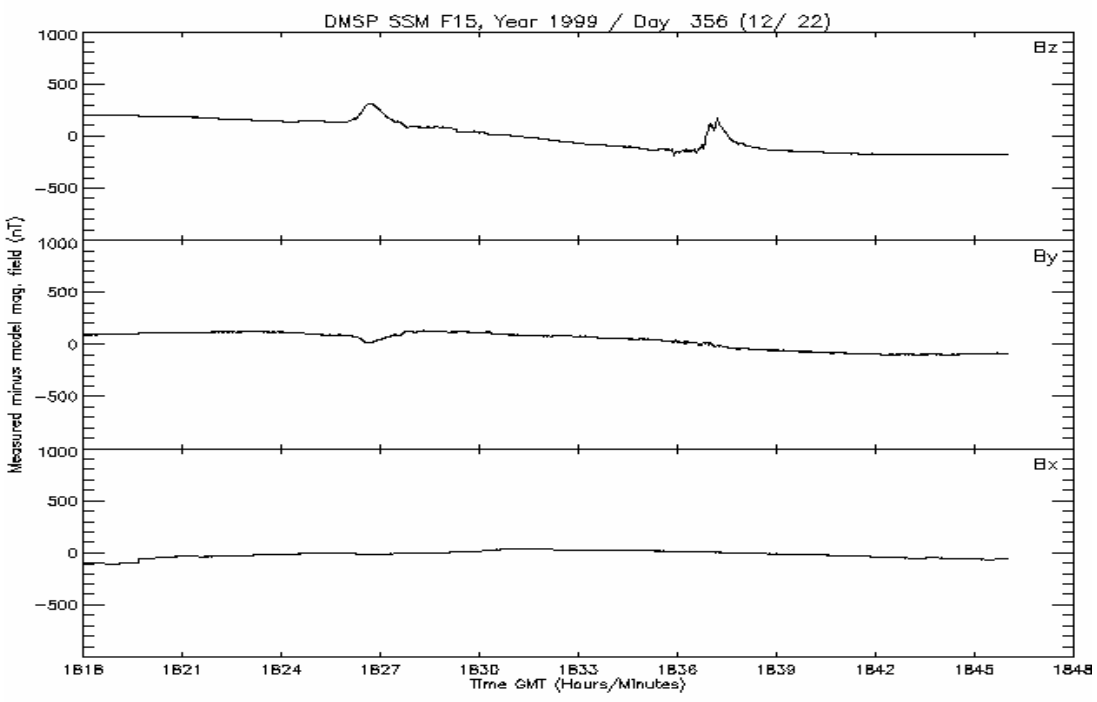

Figure 3.1. IDL graphical output of SSM data.

away from the magnetic equator using equation 2.3. One advantage of the DMSP satellite is that this correction is not needed. I am able to pick off the magnetometer reading at the magnetic equator (usually to within ±.03 degrees of latitude). Again, I start with the five international quiet days, as defined by the International Service of Geomagnetic Indices, for each month inspected against the monthly Dst index (Figure 2.6) for assurance that the day is "Dst quiet". The quiet days used are listed in Table 3.6. Days marked with an asterisk are not considered internationally quiet. During these days some magnetic storming is present and, as a result, I chose a more "Dst-quiet" day to compensate.

3.3.1 Finding the Magnetometer Reading at the Magnetic Equator

Dst measures magnetic field changes at the magnetic equator due to the storm-time ring current where these changes are in the plane parallel to the ground. Once the five quietest days are found for each month, the next step is to find the time the satellite crosses the magnetic equator. This happens twice per orbit; with an ascending (traversing northward from southern to northern latitudes) and descending (traversing southward from northern to southern latitudes) pass. I compute separate Sq values for ascending and descending passes since the orbits traverse the daytime terminator. The ascending pass occurs in darkness while the sun shines on the descending pass. Since the E-region dynamo is stronger in the day than at night, calculating separate ascending and descending solar quiet values provides an improved accounting of the Sq current system.

To find the time the satellite crosses the magnetic equator I turned to the Coupled Ion Neutral Dynamics Investigation (CINDI) which is a NASA sponsored "Mission of

Opportunity" conducted by the University of Texas at Dallas (UTD). UTD's DMSP data distribution website (http://cindispace.utdallas.edu/DMSP) allows for easy manipulation of DMSP data for each satellite. Table 3.2 shows a portion of a dataset I used for finding the times F-15 crossed the magnetic equator. As shown, the magnetic latitude, labeled MLAT, goes to zero at a time of 45300 seconds UT. This particular pass corresponds to a descending pass since when looking back in time the magnetic latitude values are positive, that is, coming from the northern hemisphere and into the southern hemisphere (MLAT values are negative with increasing time).

3.3.2 The Final Solar Quiet Monthly Value

After recording time of magnetic equator crossing, I then look to the data files created by IDL to find the corresponding Delta By magnetometer reading at 45300 seconds (Table 3.3). Delta By is used since the Y-component of the SSM's coordinate system is always approximately parallel to the ground. Variations in the magnetic field due to the storm-time ring current are mostly (not perfectly aligned with the magnetic meridian, therefore, some Z component effect) along the DMSP's Y-axis at the magnetic equator crossing. Also, the delta prefix is added to denote the subtraction of the Earth's main magnetic field via the IGRF model. Once all the magnetometer readings for each equator crossing are recorded, I then tabulate the data in an Excel spreadsheet. An example of the spreadsheet is shown in Table 3.4. For each quiet day there are about 14 orbits with corresponding ascending and descending passes (A and D on the spreadsheet). The magnetometer readings are then averaged. This gives an ascending and descending Sq value for that day. I then average the values of all five quiet days for a monthly

Date	Time	R	I	Alt.	GLAT	GLONG	MLAT	MLT
101005.	45264.0	1	1	848.2	-1.70	313.78	1.32	9.74
101005.	45268.0	1	1	848.2	-1.93	313.73	1.17	9.73
101005.	45272.0	1	1	848.2	-2.17	313.67	1.03	9.72
101005.	45276.0	1	1	848.2	-2.40	313.62	0.88	9.72
101005.	45280.0	1	1	848.2	-2.63	313.57	0.73	9.71
101005.	45284.0	1	1	848.2	-2.87	313.51	0.59	9.70
101005.	45288.0	1	1	848.2	-3.10	313.46	0.44	9.69
101005.	45292.0	1	1	848.2	-3.33	313.41	0.29	9.69
101005.	45296.0	1	1	848.2	-3.57	313.35	0.15	9.68
101005.	45300.0	1	1	848.2	-3.80	313.30	0.00	9.67
101005.	45304.0	2	1	848.3	-4.03	313.25	-0.16	9.66
101005.	45308.0	1	1	848.5	-4.27	313.19	-0.32	9.66
101005.	45312.0	1	1	848.6	-4.50	313.14	-0.48	9.65
101005.	45316.0	1	1	848.7	-4.73	313.09	-0.64	9.64
101005.	45320.0	1	1	848.8	-4.97	313.03	-0.80	9.64
101005.	45324.0	1	1	849.0	-5.20	312.98	-0.96	9.63
101005.	45328.0	1	1	849.1	-5.44	312.93	-1.12	9.62

Time in seconds

Magnetic latitude

Table 3.2. Time of magnetic equator crossing.

Time(sec UT)	Delta-Bx	Delta-By	Delta-Bz
45292.6	3.	11.	-29.
45293.6	3.	12.	-29.
45294.6	4.	11.	-28.
45295.6	3.	12.	-28.
45296.6	4.	11.	-29.
45298.6	20.	11.	-29.
45299.6	20.	12.	-29.
45300.6	20.	11.	-30.
45301.6	19.	12.	-29.
45302.6	20.	11.	-29.
45303.6	19.	12.	-30.

Time in seconds

Magnetometer reading

Table 3.3. Time and Delta By magnetometer reading.

January					
2000			2001		
8	A	D	5	A	D
	-52	62		-60	54
	-54	44		-61	49
	-56	31		-55	23
	-57	31		-38	24
	-58	26		-49	36
	-50	27		-48	33
	-69	48		-57	16
	-75	54		-61	12
	-76	48		-44	33
	-57	47		-35	50
	-64	48		-41	44
	-53			-43	40
				-43	32
				-61	50
Average	-60	42		-50	35

Magnetometer reading

Table 3.4. Excel spreadsheet For Sq. Magnetometer readings throughout the day.

average for that year. Finally, for a given month of the year, I combined the ascending Sq values for all four years into an average, likewise for the descending values. This method is repeated for all twelve months.

The solar quiet values for each month are plotted in the next two figures. Figure 3.2 shows the ascending solar quiet values throughout the calendar year while Figure 3.3 depicts the descending Sq signal. The years 2000 to 2003 are plotted as well as the total value which is the average of the four years. Once the solar quiet values are derived any storm-day's magnetometer readings can be used to create an F-15 satellite-derived Dst index.

3.4 Creation of a DMSP F-15 Dst Index

Now that solar quiet values (one ascending and descending) are determined for each month a DMSP derived Dst index can easily be created for the F-15 satellite. Similar to finding the solar quiet signal, on a storm day in question, I find the time the satellite passes the magnetic equator using the UTD website and the IDL derived data files. I recorded the time in seconds and the magnetometer reading for that time in the same Excel spreadsheet for that particular month. Table 3.5 shows that spreadsheet for the month of February. Shown is an example of storm days 12 and 13 February 2000. In the table the final ascending and descending Sq values for the month are at the top. I then subtracted the ascending and descending Sq values from the corresponding magnetometer readings. The descending values are then given a negative value, that is, -(D-Sq). This procedure is accomplished for both storm days.

In order to obtain the final DMSP Dst index for a given orbit, I average the time

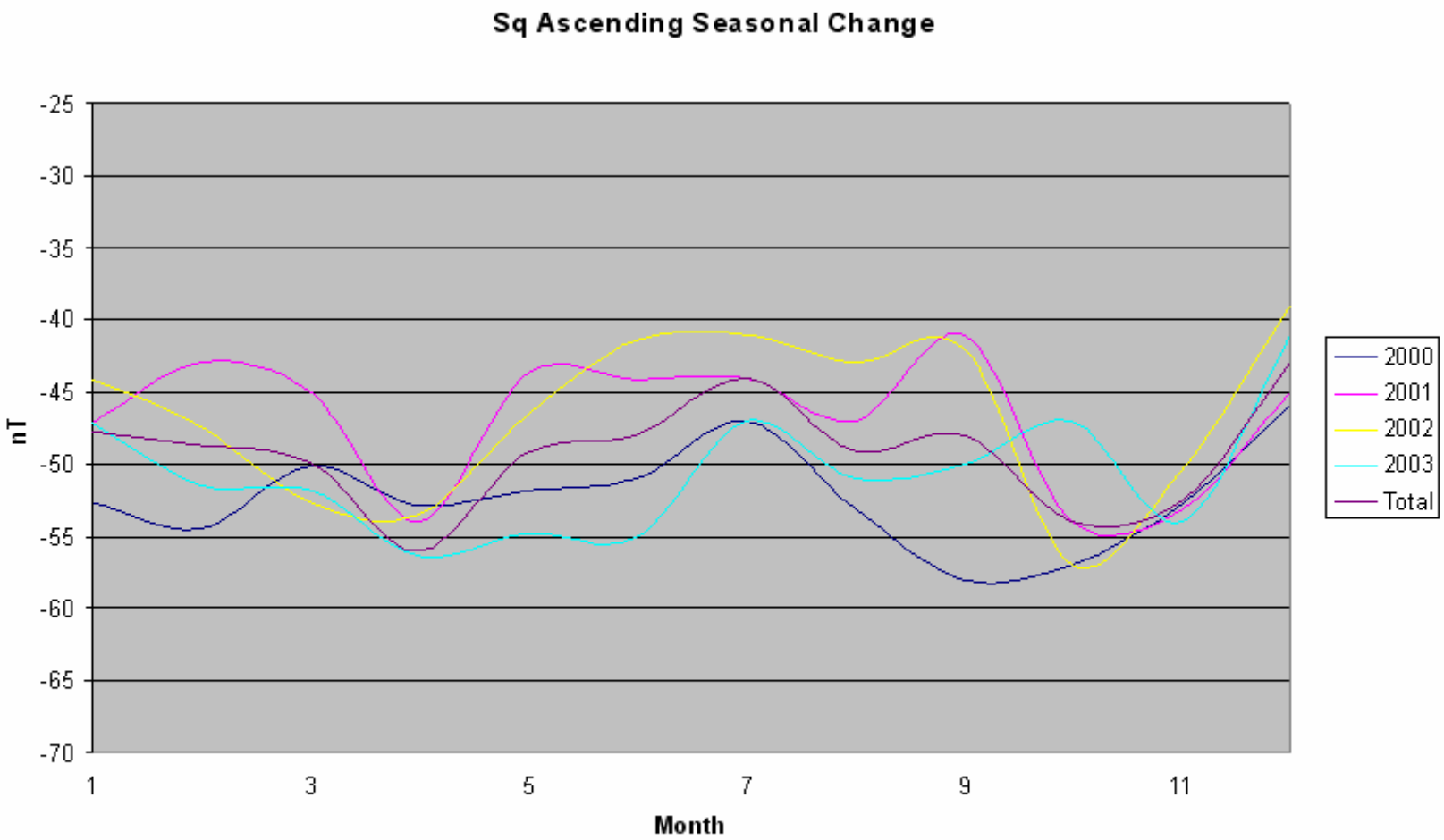

Figure 3.2. Ascending solar quiet values throughout the calendar year.

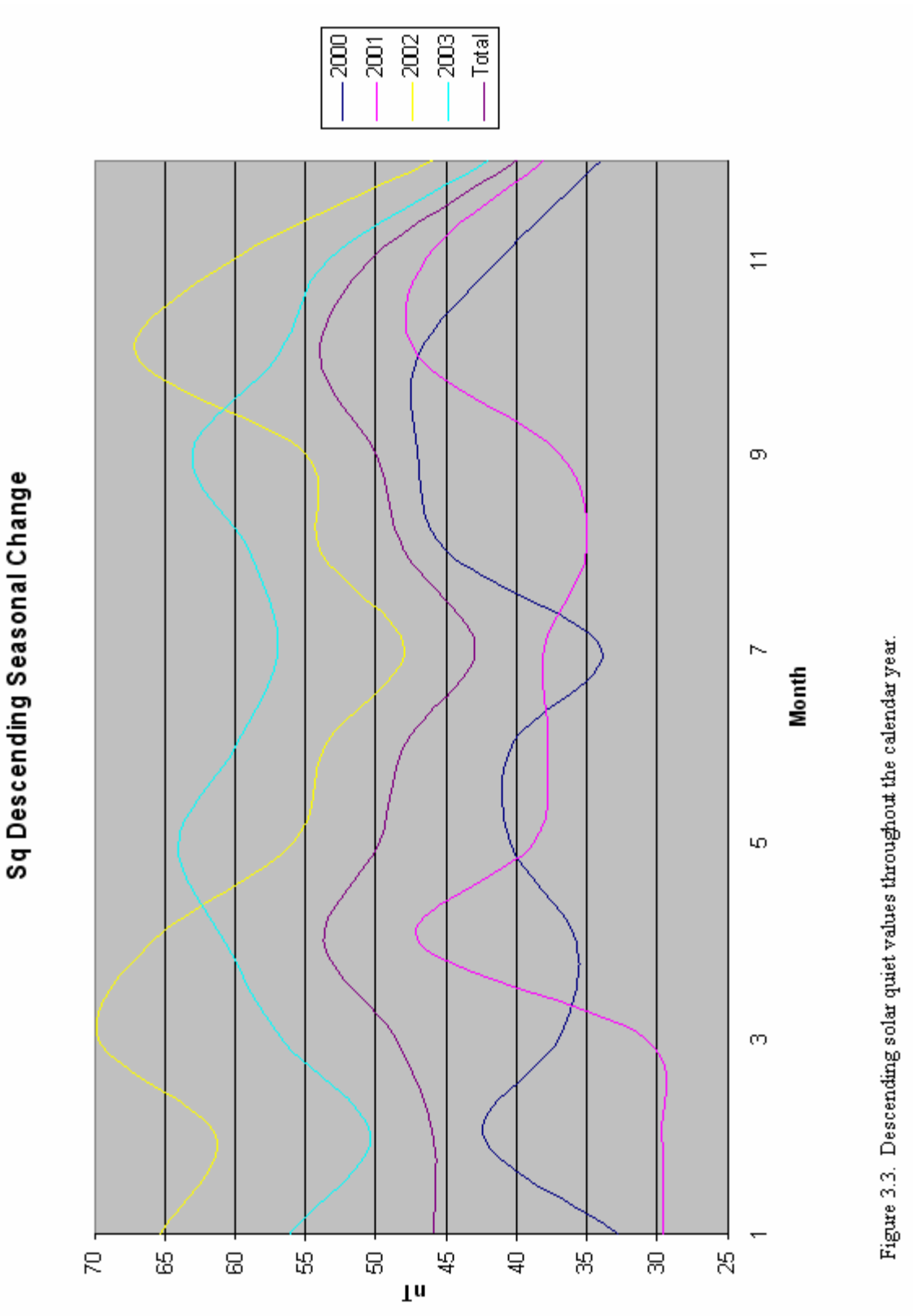

Figure 3.3. Descending solar quiet values throughout the calendar year.

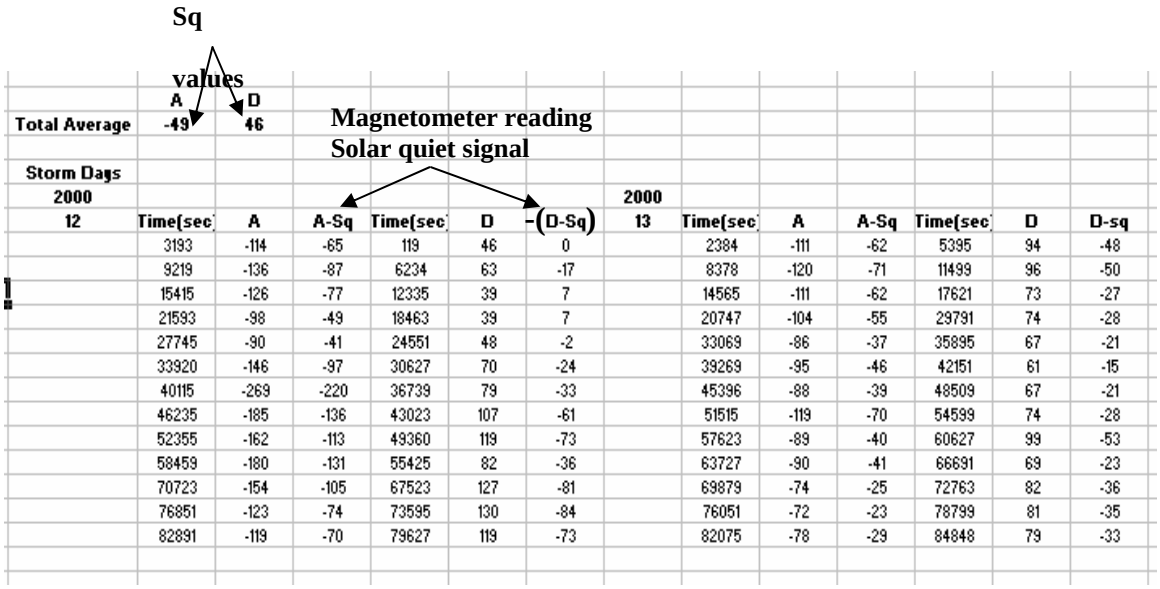

Table 3.5. Subtraction of Sq from storm-day magnetometer readings.

	2000	**2001**	**2002**	**2003**
January	8, 10*, 17, 18, 21	5*, 6, 7*, 8*, 10*	3, 4, 5, 6, 30	5*, 6, 13*, 14*, 15*
February	4, 17, 18, 19, 20	3, 4, 17, 18, 25	14, 15, 16, 23, 24*	11, 13, 23, 24, 25
March	3*, 26, 27, 28*	10*, 11, 15, 16, 17	12*, 13*, 14, 27*, 28	8, 12, 24, 25, 26
April	14, 15*, 21*, 22, 23*	21, 25, 26, 27, 30*	5, 7*, 8, 26, 27*	6, 7, 12, 13, 19
May	7, 11, 19*, 20, 21	1, 5, 21, 30, 31	1, 2*, 3*, 4*, 31	3, 4, 16, 17, 18
June	7*, 16*, 17, 25, 30	12, 22, 23, 28, 29	6*, 7*, 21*, 25*, 26*	5, 6*, 7*, 12, 13
July	5*, 6, 7, 8*, 9*	2, 7, 19*, 20, 28	2, 3, 4, 28*, 29*	8, 9, 10, 23*, 24*
August	18, 19, 20*, 25, 26	11, 15, 16, 24, 29	6, 7, 8*, 24, 25	5, 14*, 15*, 16, 31
September	9, 10, 11, 14, 22	1, 7, 9, 10, 20*	20, 23, 24, 25, 29	7, 14, 28, 29, 30
October	9, 18*, 19*, 20, 21,	6*, 7, 16*, 17, 18	19*, 20*, 21, 22, 23*	8*, 9*, 10, 11, 12
November	2, 3, 15, 16, 17	3, 13*, 14, 15*, 30	1, 8, 9, 16, 17	7*, 8, 27, 28, 29
December	14, 15, 20, 30, 31	1*, 8*, 9, 10, 11	6*, 11, 12, 13, 17	3, 18, 19, 25, 29

* Not one of the five international quiet days.

Table 3.6. The five “quiet days” used to determine the DMSP F-15 solar quiet signal.

between corresponding ascending and descending passes along with their magnetometer readings minus the Sq value. To clarify, I average the first ascending final value of the day (storm magnetometer reading minus corresponding Sq value) with the first descending final value of the day along with their times crossing the magnetic equator. Next, the second ascending/descending final values and times are averaged and so on. Also, if, for example, an ascending pass is unavailable, the corresponding descending value will not be used. The averages are shown in the center columns of Table 3.7. Also shown are the actual ground-based hourly Dst values obtained from the Kyoto website mentioned earlier.

The hourly value for the ground-based Dst was listed to correspond to the 30 minute mark between the hours. For example, the Dst value for 0200-0300 UT is listed for a time of 0230 or 9000 seconds as seen on the table. The right hand column is the list from Table 3.5 of the individual ascending and descending magnetometer values minus the corresponding solar quiet value. The data from Table 3.7 is then plotted to create a graph like that of Figure 2.6 with the addition of my F-15 Dst and the individual ascending and descending values. I plotted a Dst trace for a magnetic storm for each of the twelve months of the year with the exception of two storms for the month of November. Figures 3.4 - 3.16 show these Dst indices for each of these storms.

Actual Dst			DMSP Dst			Actual				
12	1800	-24	Average (A-sq+D-Sq)/2			12	A		D	
	5400	-38	12	1656	-32		3193	-65	119	0
	9000	-42		7727	-52		9219	-87	6234	-17
	12600	-60		13875	-35		15415	-77	12335	7
	16200	-47		20028	-21		21593	-49	18463	7
	19800	-24		26148	-21		27745	-41	24551	-2
	23400	-30		32274	-60		33920	-97	30627	-24
	27000	-33		38427	-126		40115	-220	36739	-33
	30600	-29		44629	-98		46235	-136	43023	-61
	34200	-67		50858	-93		52355	-113	49360	-73
	37800	-98		56942	-83		58459	-131	55425	-36
	41400	-133		69123	-93		70723	-105	67523	-81
	45000	-108		75223	-79		76851	-74	73595	-84
	48600	-91		81259	-71		82891	-70	79627	-73
	52200	-105	13	90290	-55	13	88784	-62	91795	-48
	55800	-96		96339	-60		94778	-71	97899	-50
	59400	-103		102493	-44		100965	-62	104021	-27
	63000	-110		111669	-41		107147	-55	116191	-28
	66600	-109		120882	-29		119469	-37	122295	-21
	70200	-102		127110	-30		125669	-46	128551	-15
	73800	-95		133353	-30		131796	-39	134909	-21
	77400	-89		139457	-49		137915	-70	140999	-28
	81000	-84		145525	-46		144023	-40	147027	-53
	84600	-77		151609	-32		150127	-41	153091	-23
13	86400	-61		157721	-30		156279	-25	159163	-36
	90000	-46		163825	-29		162451	-23	165199	-35
	93600	-55		169862	-31		168475	-29	171248	-33
	97200	-55								
	100800	-55								
	104400	-53								
	108000	-54								
	111600	-54								
	115200	-57								
	118800	-55								
	122400	-55								
	126000	-55								
	129600	-57								
	133200	-57								
	136800	-58								
	140400	-50								
	144000	-41								
	147600	-35								
	151200	-32								
	154800	-37								
	158400	-41								
	162000	-35								
	165600	-31								
	169200	-29								

F-15 Dst value

Time and magnetometer reading minus Sq

Actual Ground-based Dst

Table 3.7. Actual and F-15 Dst spreadsheet.

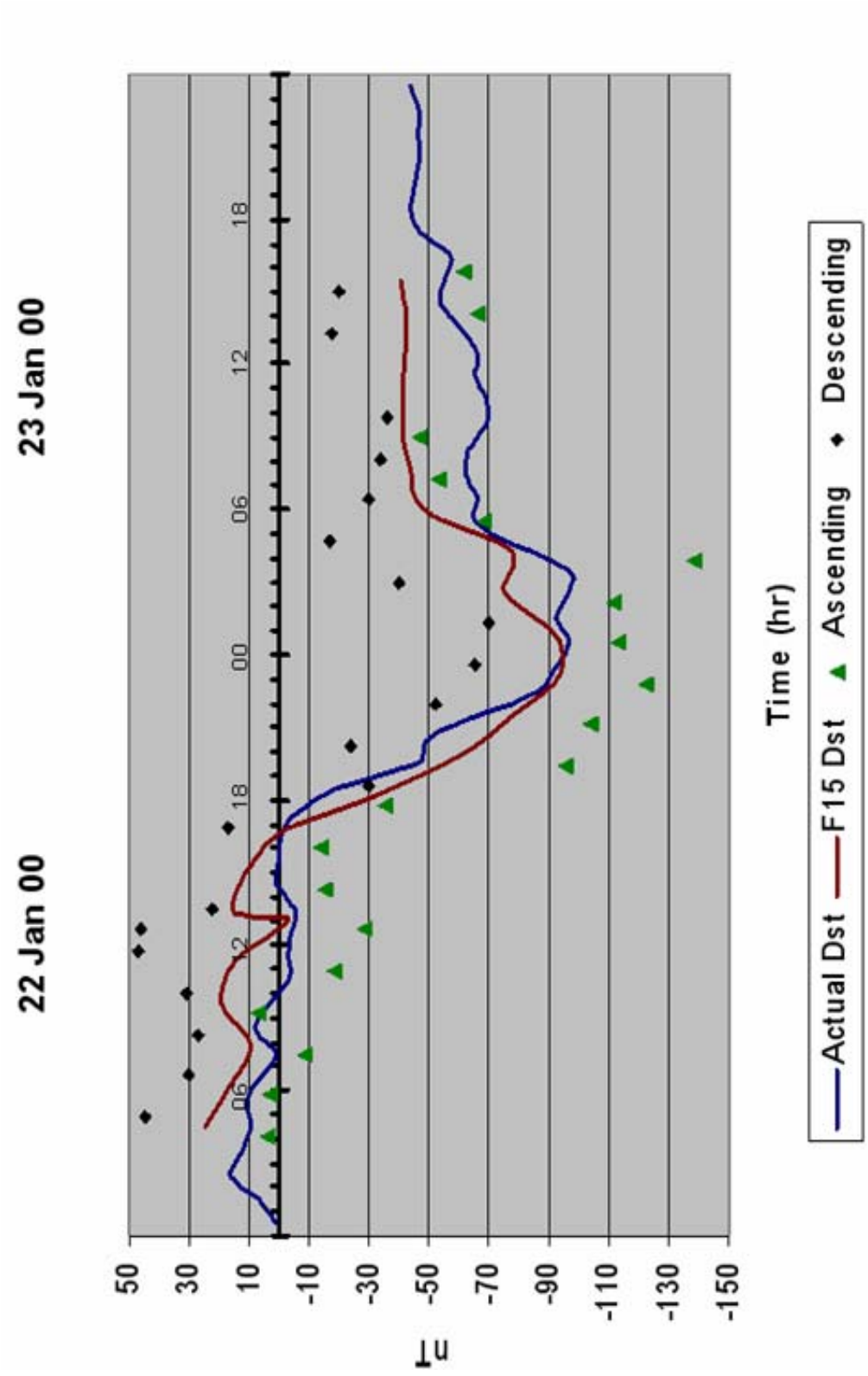

Figure 3.4. Actual vs. DMSP F-15 Dst for 22-23 January 2000.

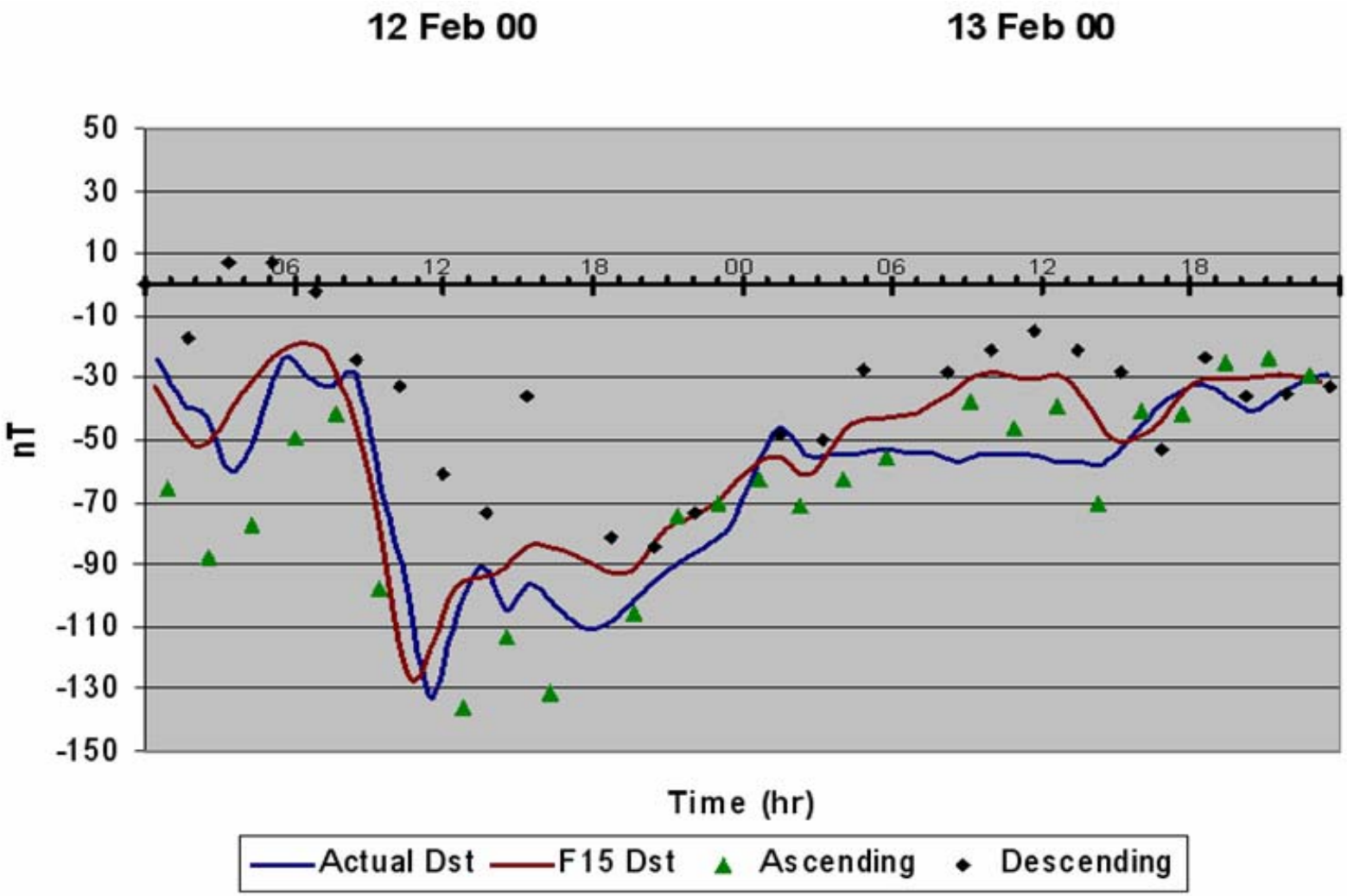

Figure 3.5. Actual vs. DMSP F-15 Dst for 12 -13 February 2000.

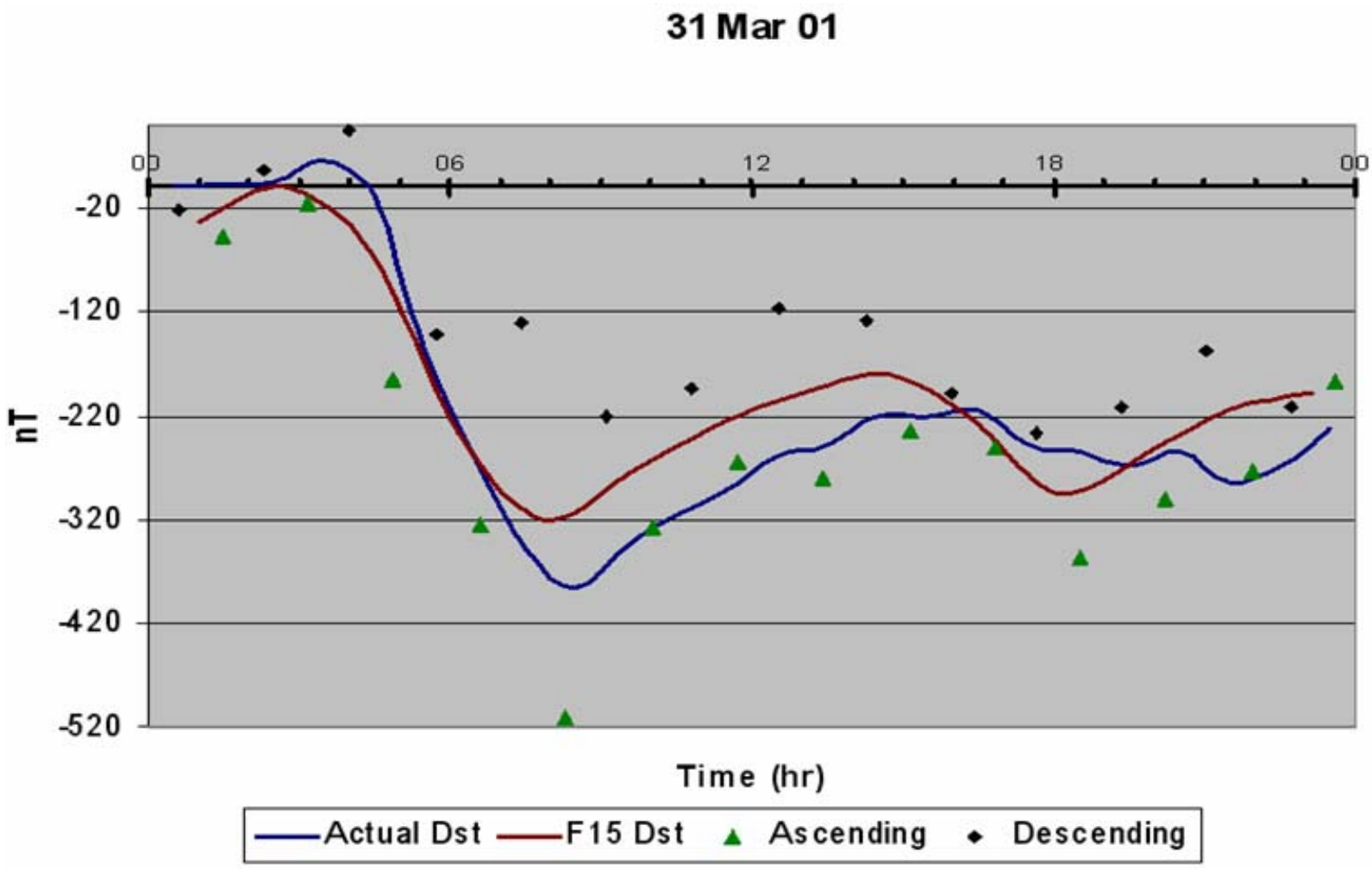

Figure 3.6. Actual vs. DMSP F-15 Dst for 31 March 2001.

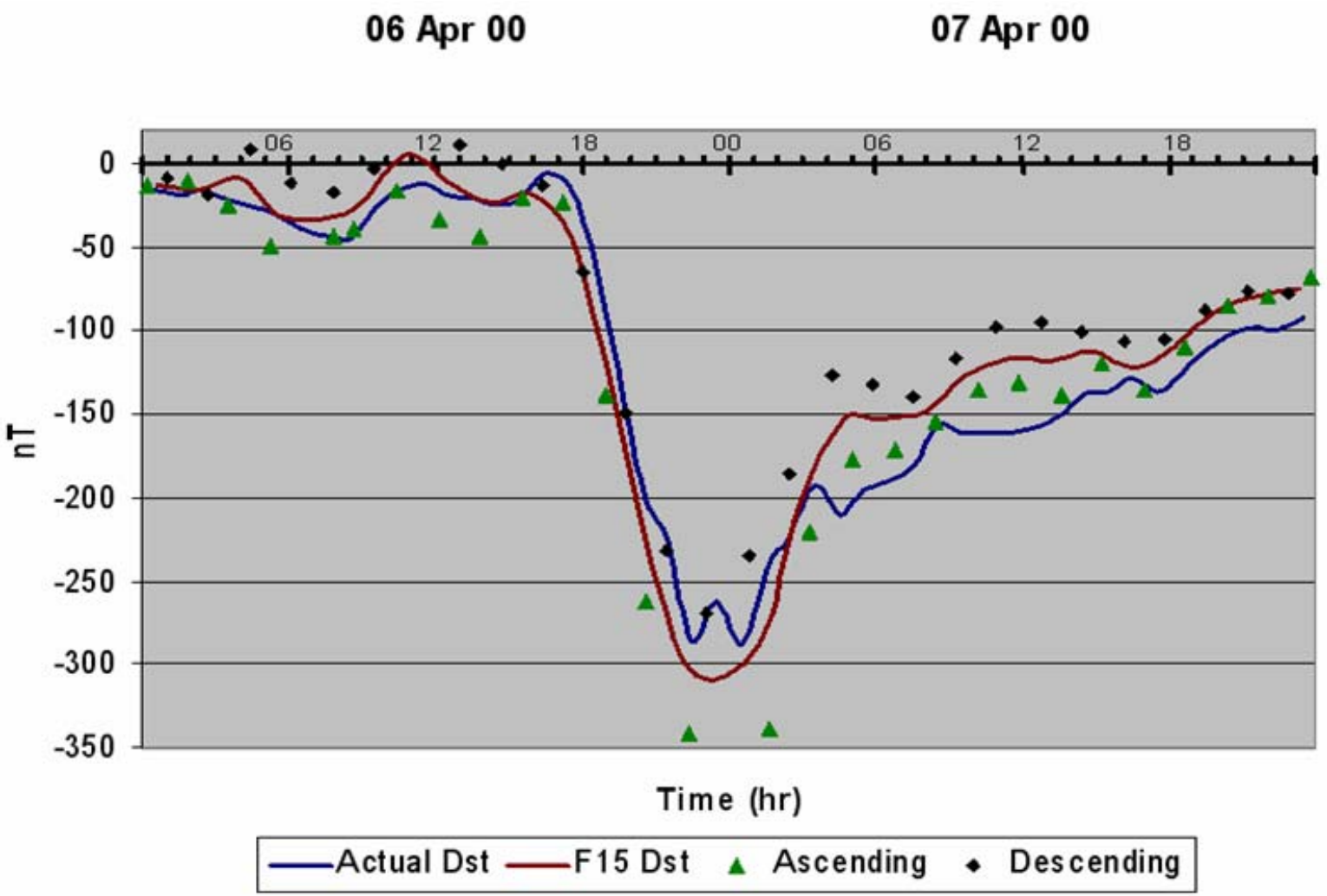

Figure 3.7. Actual vs. DMSP F-15 Dst for 06-07 April 2000.

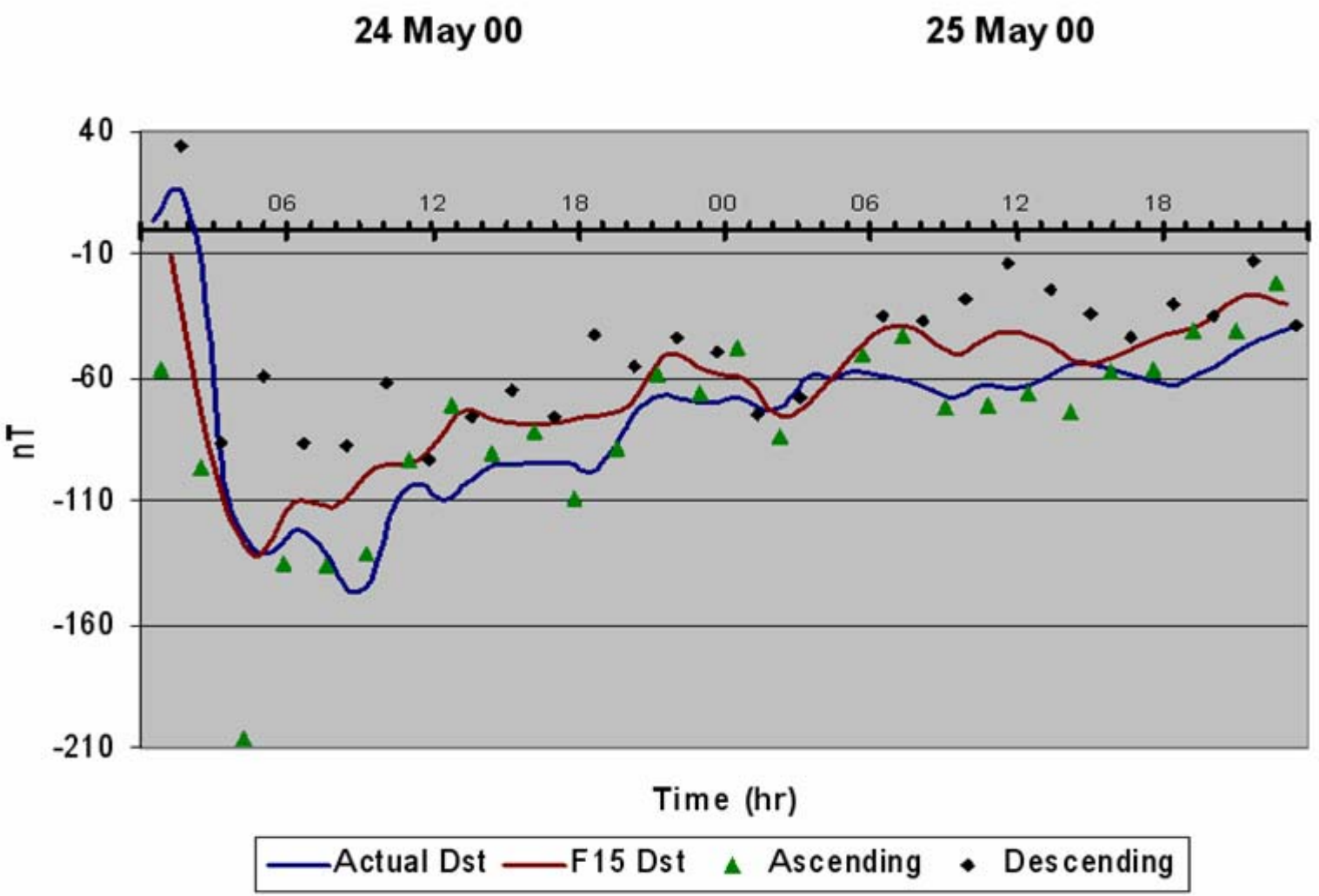

Figure 3.8. Actual vs. DMSP F-15 Dst for 24-25 May 2000.

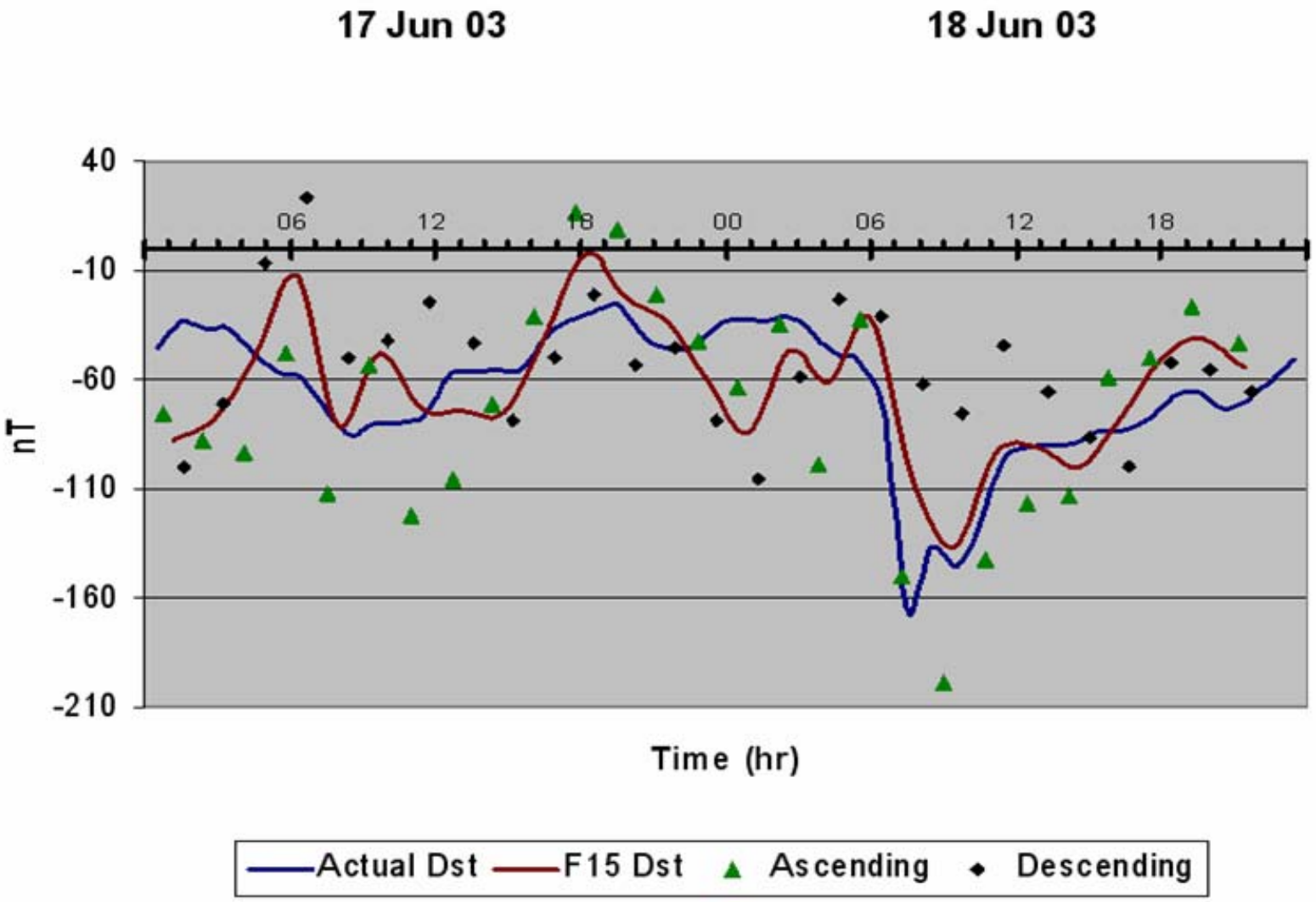

Figure 3.9. Actual vs. DMSP F-15 Dst for 17-18 June 2003.

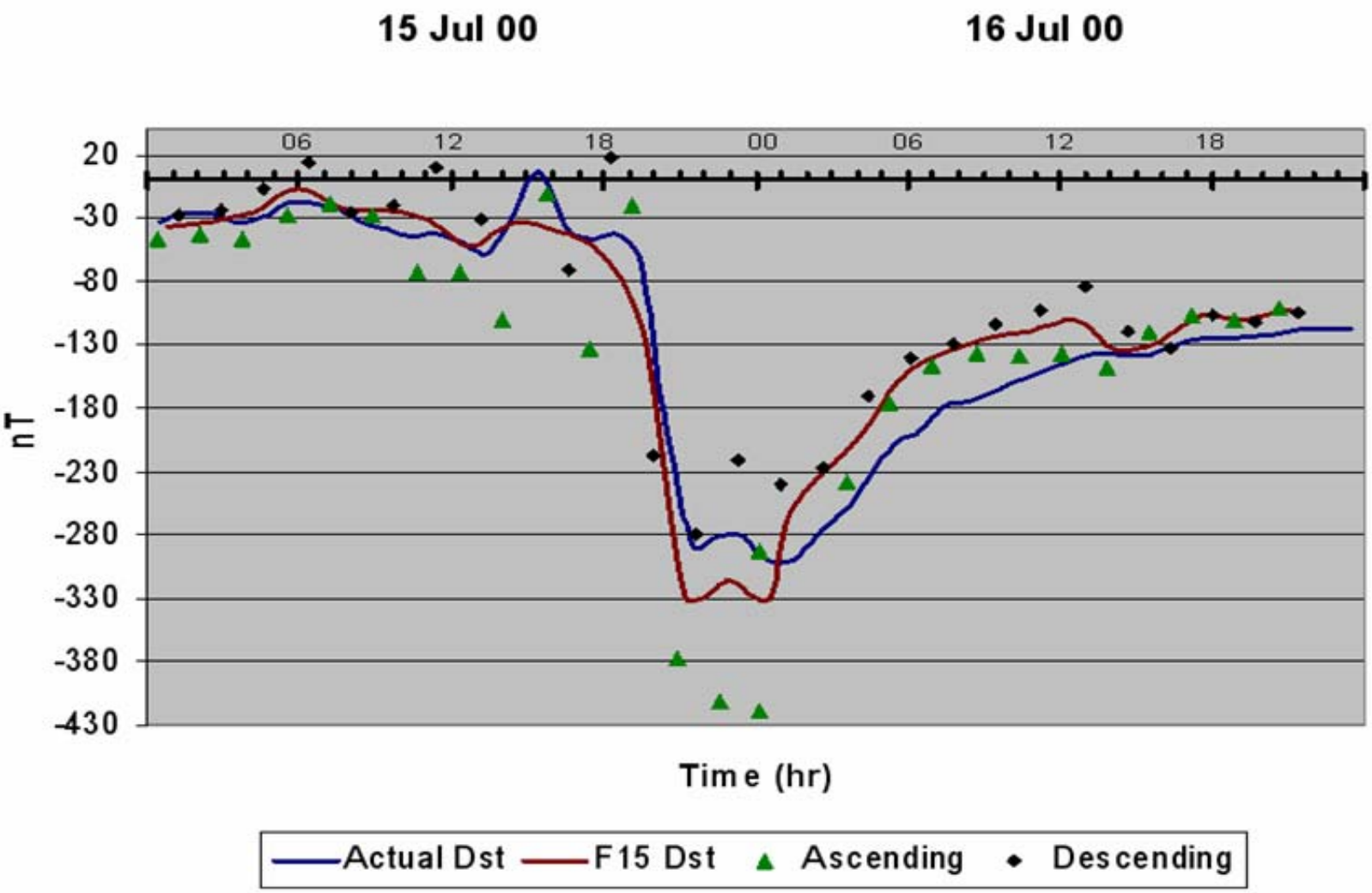

Figure 3.10. Actual vs. DMSP F-15 Dst for 15 -16 July 2000.

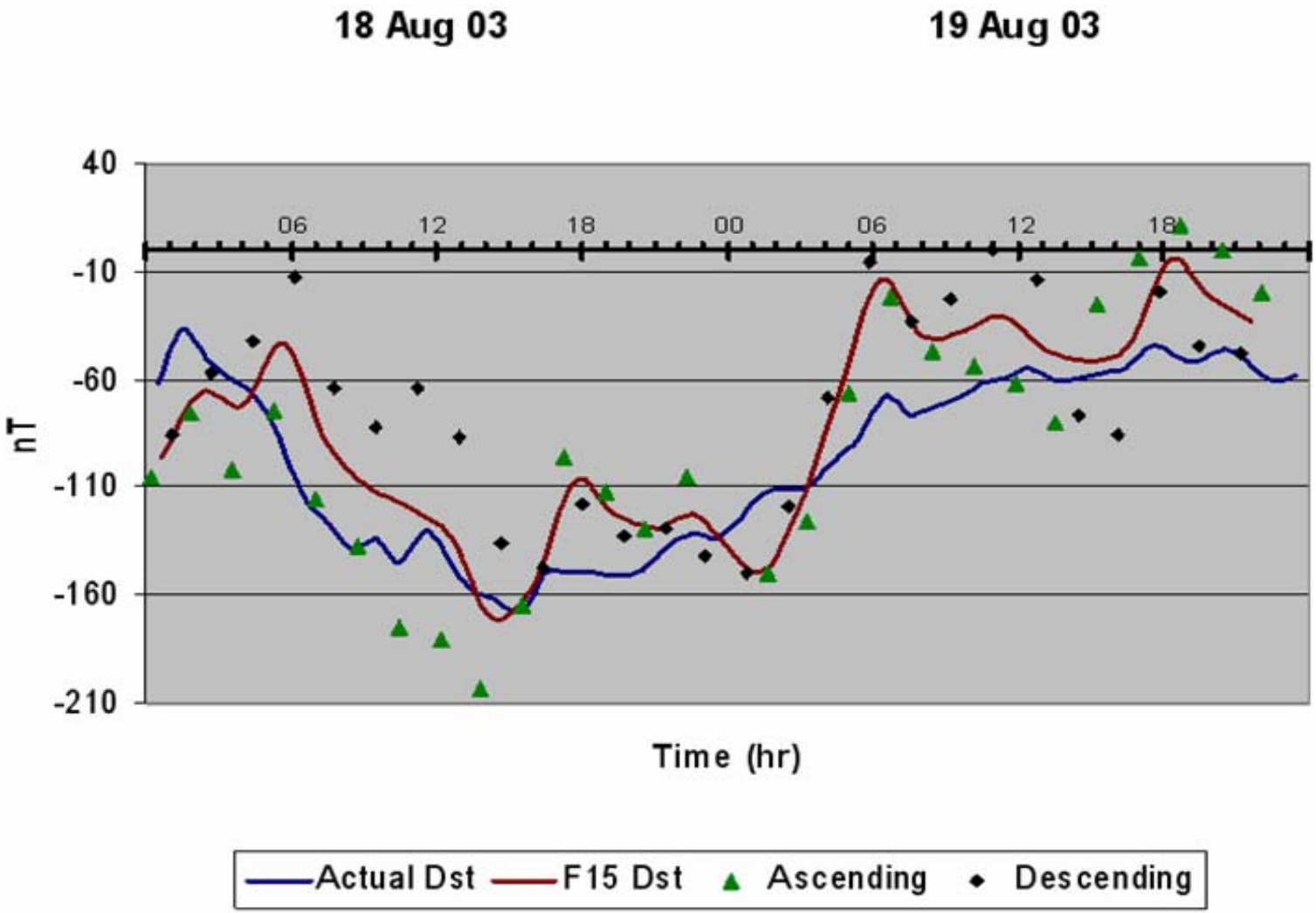

Figure 3.11. Actual vs. DMSP F-15 Dst for 18-19 August 2003.

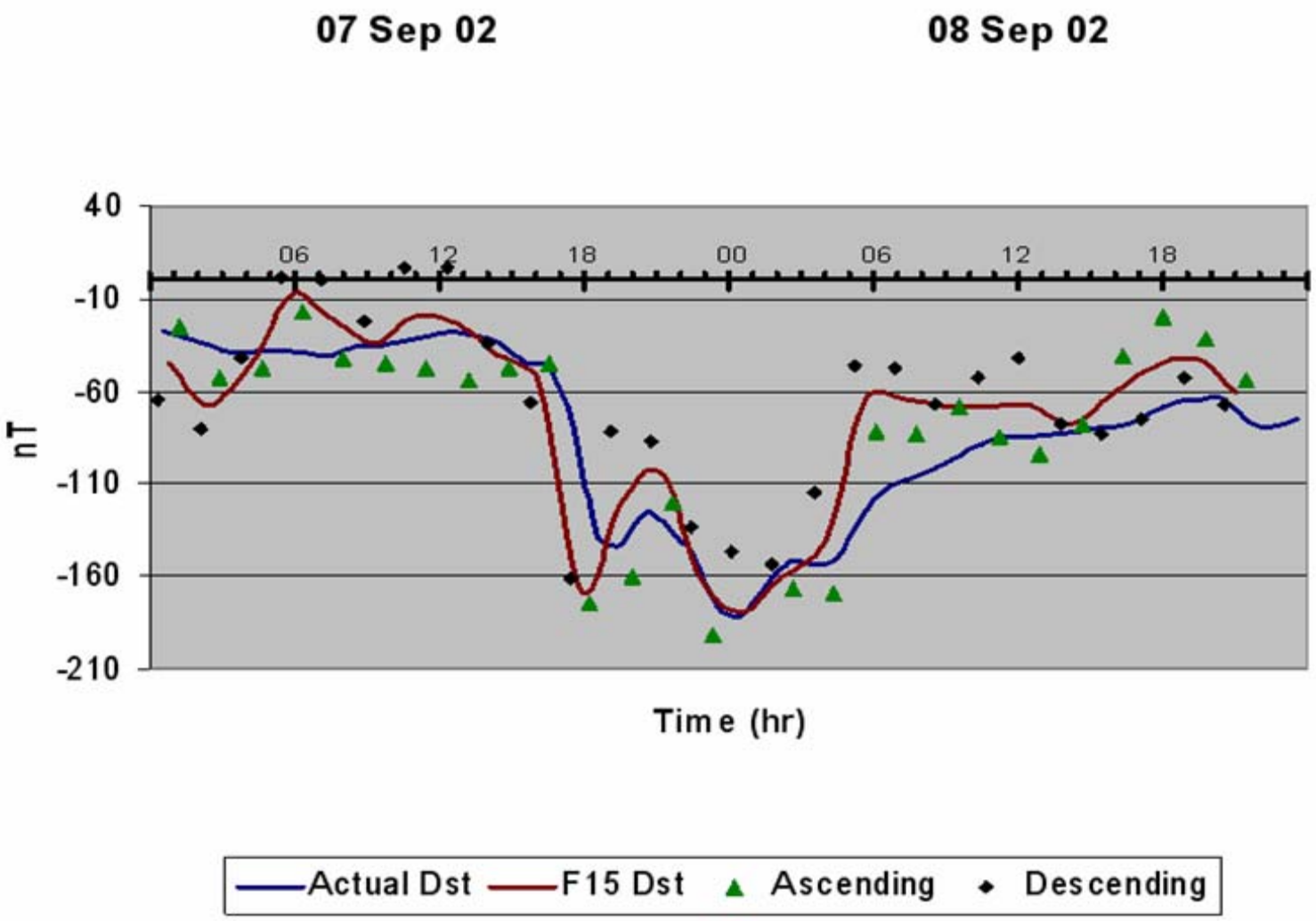

Figure 3.12. Actual vs. DMSP F-15 Dst for 07-08 September 2002.

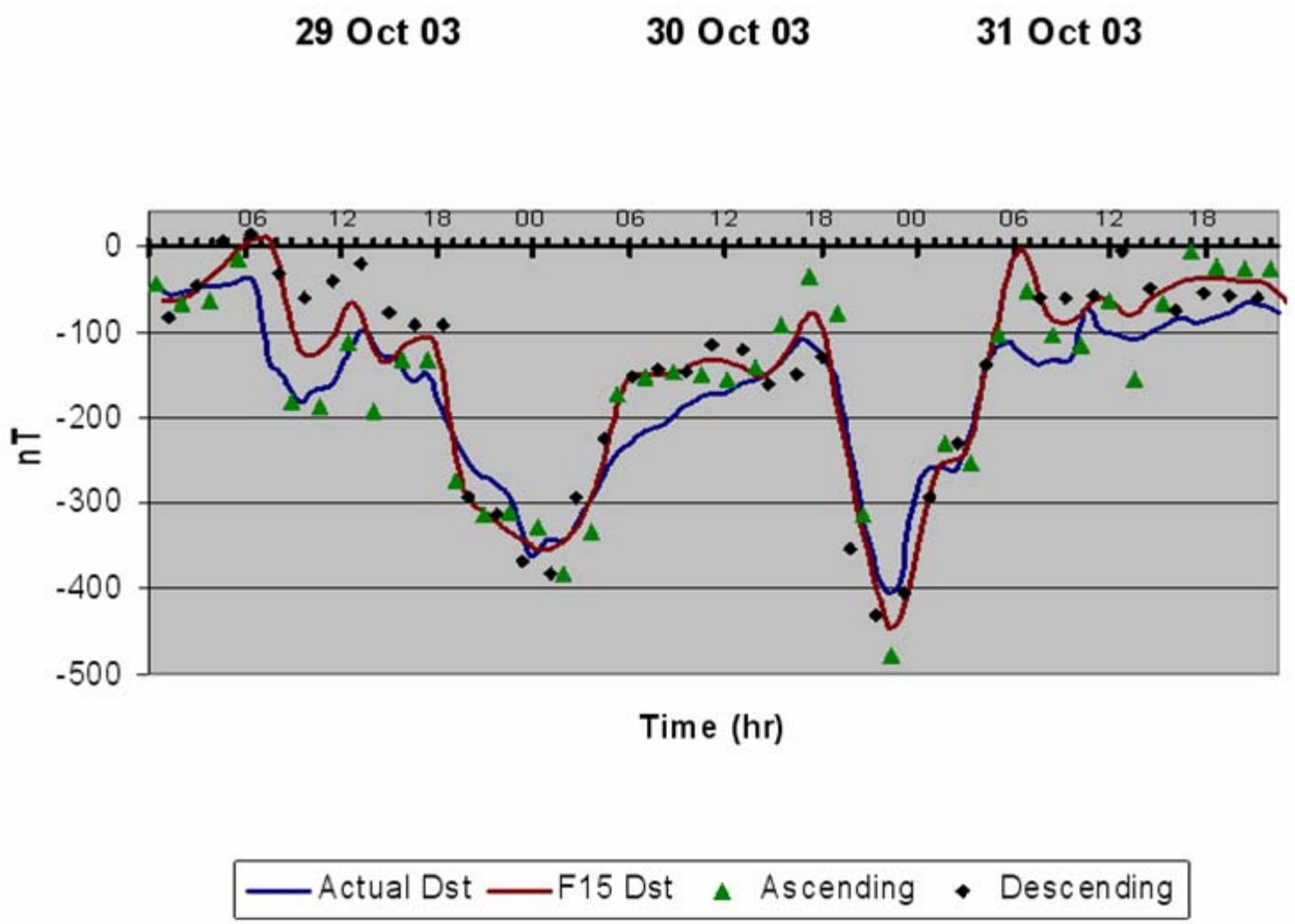

Figure 3.13. Actual vs. DMSP F-15 Dst for 29-31 October 2003.

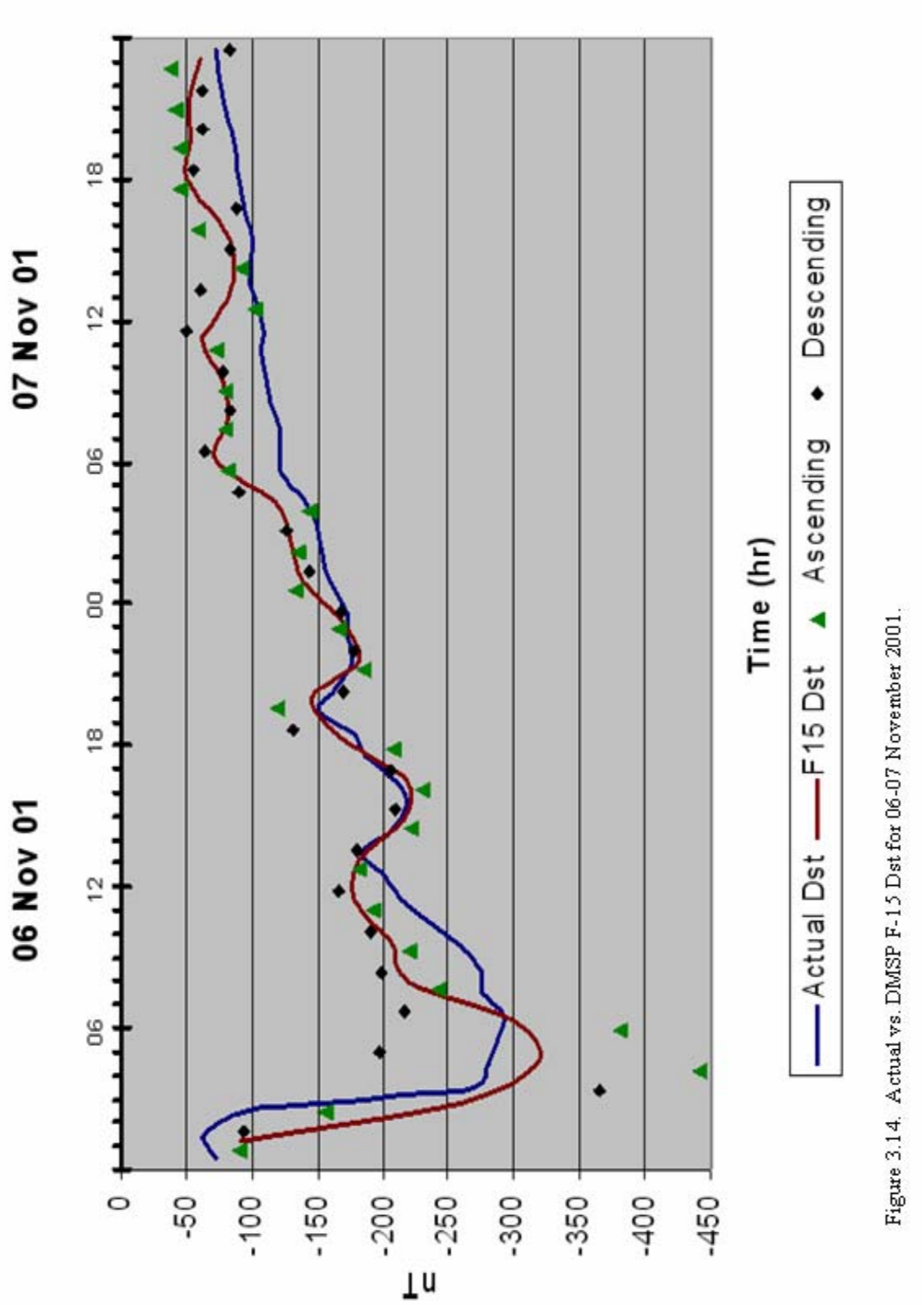

Figure 3.14. Actual vs. DMSP F-15 Dst for 06-07 November 2001.

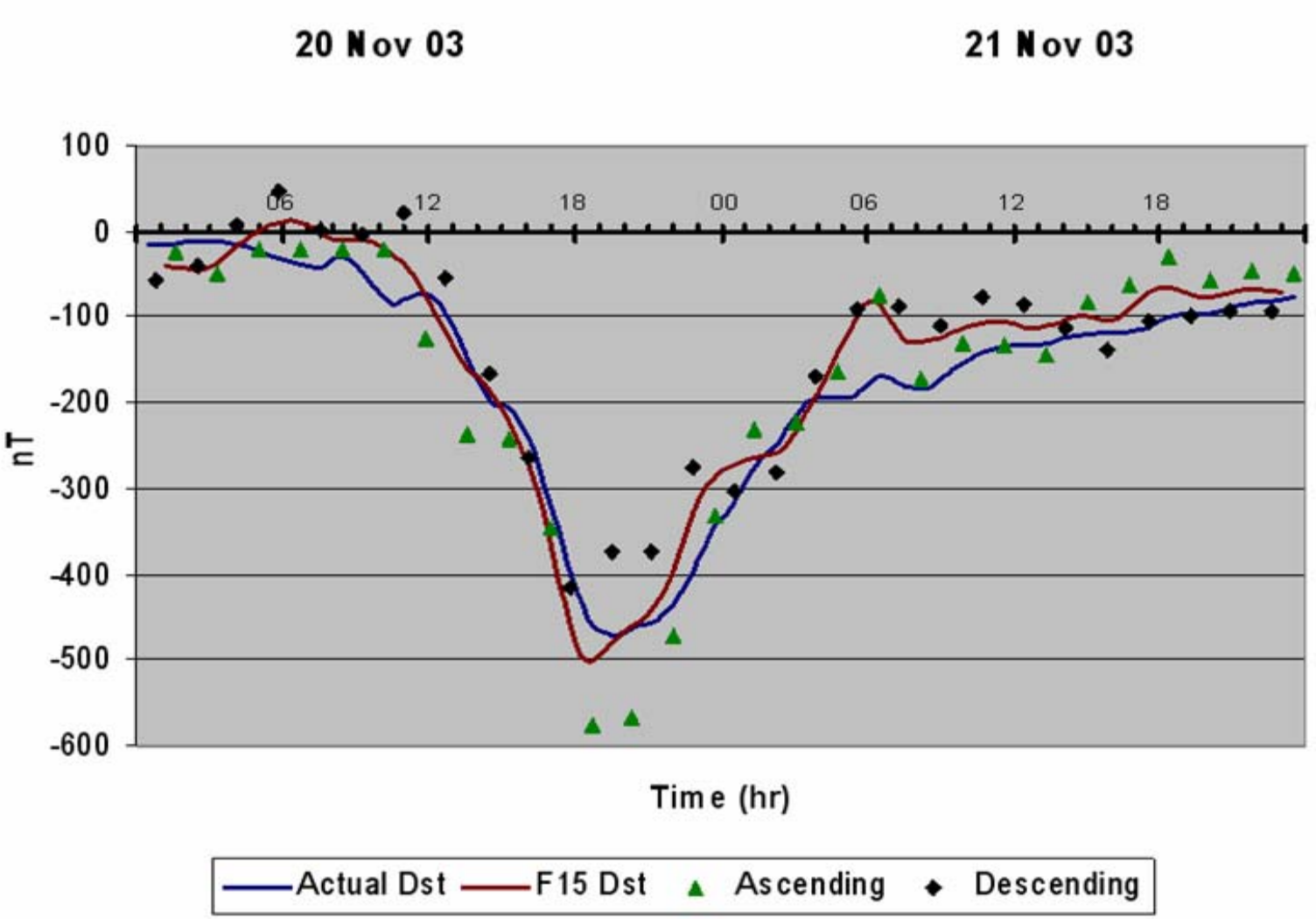

Figure 3.15. Actual vs. DMSP F-15 Dst for 20-21 November 2003.

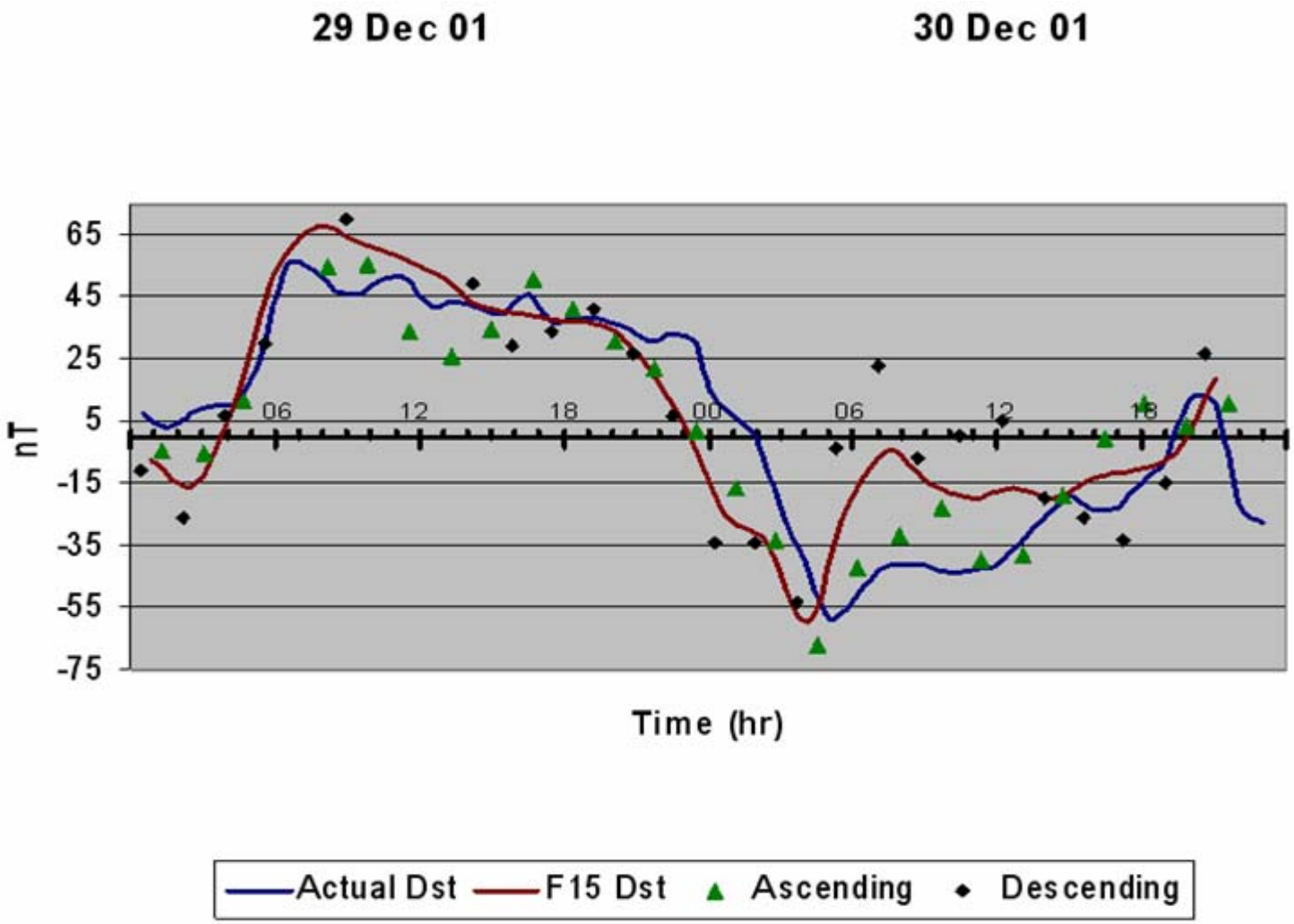

Figure 3.16. Actual vs. DMSP F-15 Dst for 29-30 December 2001.

IV. Results and Future Work

4.1 Results

This section discusses the comparison between the actual ground-based Dst index and my derived DMSP Dst for the F-15 satellite. A statistical comparison is presented comparing the two Dst curves. I'll also scrutinize the solar quiet signal results as well as the Sq ascending and descending plots of Figures 3.2 and 3.3. Finally, advantages and limitations of my method for finding Sq and a final DMSP Dst are be discussed.

4.1.1 Comparison of Actual Ground-Based Dst to DMSP F-15 Derived Dst

The resulting plots in Figures 3.4 – 3.16 show a good comparison between the ground-based Dst values and the DMSP F-15 derived trace. Although in some cases the curves are slightly out of phase, the shapes of the graphs mostly agree with each other. The phase differences could be a result of plotting the hourly ground-based Dst value at half past each UT hour. As stated in section 3.4, my DMSP derived Dst values are plotted at a time halfway between the two magnetic equator crossings (one descending, one ascending) used to derive that index value. In all cases the DMSP derived Dst shows a clear sudden commencement, main phase, and recovery phase that is shown in the traditional Dst trace. Table 4.1 provides the statistical analysis of the storms.

4.1.2 Statistical Analysis Between Ground-Based and the F-15 Derived Dst

Statistical analysis between the two Dst curves also shows good agreement. Analysis of the curves was accomplished using two spreadsheet programs. The graphs

were made using Excel. Once the graphs were made I analyzed the difference fields, DMSP derived Dst minus the actual ground-based value, between the two curves and performed a paired *t*-test. This required me to interpolate the two time series (DMSP-derived and official Dst) to obtain pairs of values valid at the same time. I used Origin 6.1 to accomplish this interpolation. For consistency with the official Dst cadence, I chose to interpolate at one-hour intervals.

Table 4.1 is an analysis of the difference between the entire curves. The table shows an analysis for each storm using the differences between data points of the curves selected once every hour. Interpolating data points once every hour gives 48 data points (two days) for all the months except for March (1 day, 24 data points) and October (3 days, 72 data points). Notice that all of the mean differences have a positive value. A positive mean difference indicates that the DMSP Dst has smaller (negative) values than the ground-based Dst. That is, the DMSP Dst shows a slightly weaker magnetic storm.

This result is counter-intuitive to the fact that the satellite, being 850 kilometers closer to the ring current than the ground-based observatories, should report a stronger storm. This may be partly explained by the fact that, as the F-15 satellite orbits the planet, the By axis does not align perfectly with a given magnetic meridian. Adding the delta Bz to the results could recover some of this error.

Table 4.1 also lists the time series statistics and data using a paired *t*-test. Given two paired sets, DMSP and observed Dst values, the paired *t*-test determines whether they differ from each other in a significant way under the assumptions that the paired differences are independent and identically normally distributed. Data from the paired t-test shows the standard difference error and a 95% confidence interval for the mean value

	Time Series Statistics							
	Difference (DMSP - Observed)		Mean		Standard Deviation		Data from Paired t-test	
	Mean	Stand Dev.	DMSP	Observed	DMSP	Observed	Stand Diff. Error	95% Conf. Interval
January	8.46	11.82	-32.75	-41.21	38.06	37.13	1.71	5.03 to 11.88
February	7.44	11.9	-53.96	-61.40	26.28	27.72	1.72	3.99 to 10.89
March	18.22	42.48	-197.38	-215.67	90.09	118.58	8.67	0.38 to 36.21
April	6.54	22.93	-104.92	-111.42	87.01	82.13	3.30	-0.13 to 13.13
May	11.06	15.44	-64.90	-75.96	26.74	31.92	2.23	6.59 to 15.54
June	2.02	24.54	-63.48	-65.56	27.25	30.10	3.54	-5.03 to 9.20
July	5.3	25.21	-115.71	-121.04	90.12	89.52	3.64	-1.98 to 12.65
August	14.92	22.19	-81.23	-96.15	46.18	41.20	3.21	8.46 to 21.37
September	7.45	19.86	-74.63	-82.00	45.79	44.73	2.87	1.60 to 13.15
October	22.13	35.76	-147.96	-170.11	112.26	91.86	4.21	13.74 to 30.56
November (01)	13.32	28.26	-143.73	-157.02	74.93	66.09	4.08	5.08 to 21.51
November (03)	14.72	29.91	-151.38	-166.10	136.71	129.39	4.32	6.02 to 23.44
December	1.63	17.8	6.77	5.15	34.31	34.98	2.57	-3.54 to 6.79

Table 4.1. Statistical analysis of DMSP derived Dst minus observed value and paired *t*-test results.

of the paired differences. The discrepancy of the confidence interval about the mean depends on the size and variability of the sample.

The standard deviations and the high end of the confidence intervals of Table 4.1 for all months of storms are in the low tens of nanoteslas. In section 2.7 I totaled the factors for error to be about a few hundred nT if all acted in concert and operated in the same direction. The standard deviations and confidence intervals are well within the total error value by one order of magnitude. This illustrates very good agreement between my DMSP derived Dst and the existing ground-based storm index.

4.1.3 Results of the DMSP F-15 Solar Quiet Signal

Figures 3.2 and 3.3 show the solar quiet signal for the ascending and descending passes of the DMSP F-15 satellite. Figure 4.1 shows the solar cycle for the past ten years as well as a forecast of the progression out to 2008. The solar cycle from 2000 to 2004, corresponding to solar maximum (the years of my research data), shows a complicated pattern. While April of 2000 was declared the peak solar (sunspot) maximum, there is actually a dip in the sunspot values then another peak occurring at the beginning of 2002. Figure 4.1 shows these two peaks and valley between them. The large sunspot count is probably accounted for in the descending, daytime, trace (Figure 3.3) reflecting the solar quiet current system. The Sq current system has much less of an effect during the nighttime, ascending, satellite pass resulting in lower values in Figure 3.2. Although the absolute values of the ascending monthly Sq values are lower than that of the descending Sq values they should be closer to zero. Some residual ring current component is

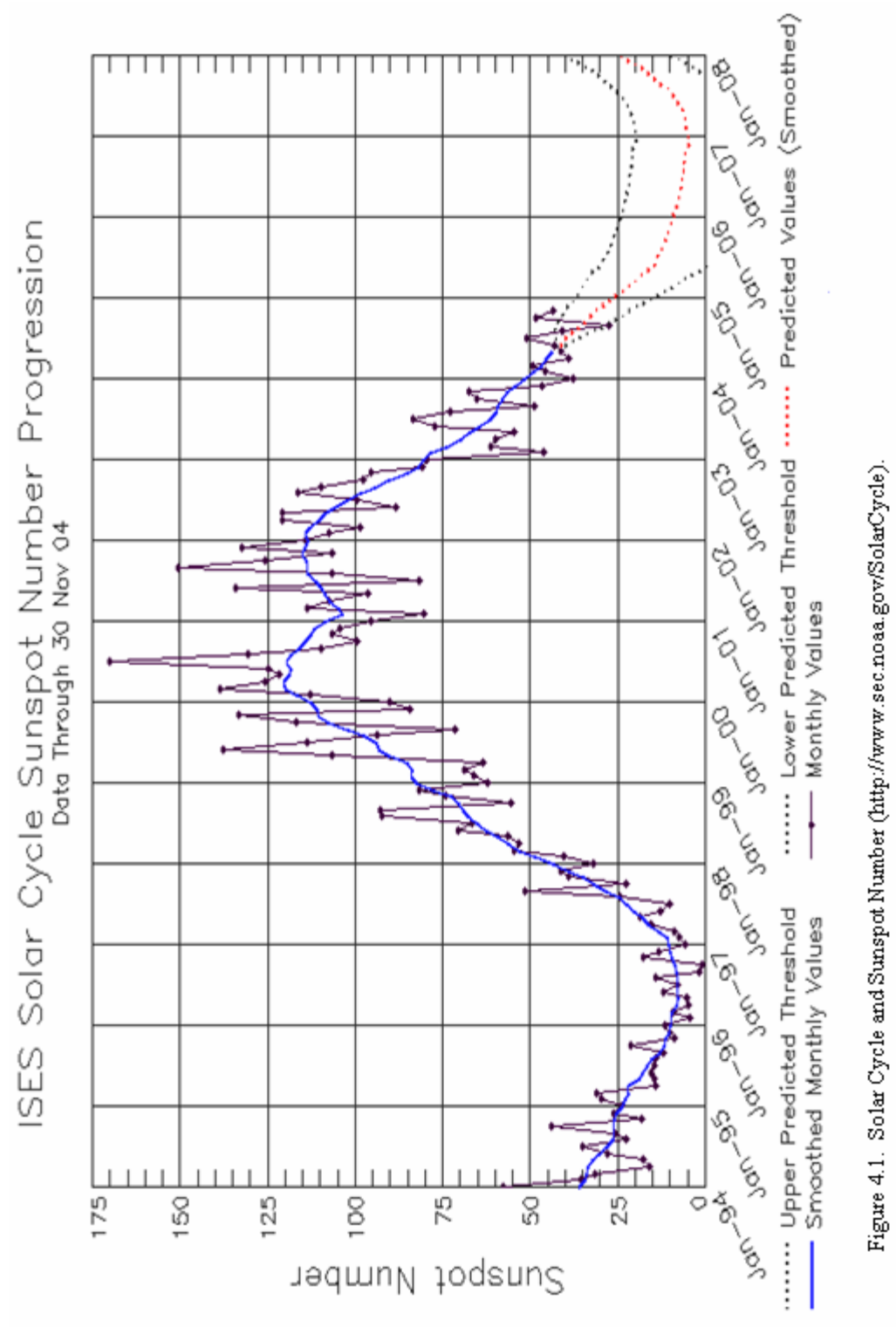

Figure 4.1. Solar Cycle and Sunspot Number (http://www.sec.noaa.gov/SolarCycle).

probably present in the ascending Sq values. My solar quiet signal does, somewhat, agree with the solar cycle.

On the descending Sq plot, January-March 2000 does have the largest negative values. The high Sq values for 2003 is somewhat mysterious, but could be explained by some large magnetic storms throughout the year making it tough to find a quiet signal. Interestingly, Figures 3.2 and 3.3 both show strong values during the spring and fall and weaker values during the northern hemisphere summer months. This may be explained by direct sunlight at the equator during the vernal and autumnal equinoxes increasing the conductivity of the ionosphere. Also, thermospheric winds, responsible for the Sq current system, are stronger during this time period.

4.2 Limitations of the DMSP F-15 Derived Dst

Even with the good results of the DMSP derived Dst there are a some limitations to calculating the index from the F-15 satellite. First, my solar quiet signal is averaged for all four years for each particular month. This results in a solar quiet signal that is not solar cycle dependent. Also, the satellite's orbit is closer to the ring current than the magnetometers on the ground. Thus, as stated in the factors for error section, delta By is estimated to be about six percent smaller at the ground-based magnetometers on the Earth's surface than at an F-15 altitude of about 850 km. Also, as the F-15 satellite orbits the planet the By axis does not align perfectly with a given magnetic meridian. As stated previously, adding delta Bz could help to offset this limitation.

Another limitation is the averaging I made between the ascending and descending magnetic equator passes. The satellite takes approximately 90 to 100 minutes to orbit the

planet. As a result, the time between the ascending and descending passes are 45 to 50 minutes apart. Another difference between these two passes is that the ascending pass happens in darkness while the descending pass occurs in the sunlight. Therefore, I'm averaging two magnetometer values which are taken at two different times. Naturally, this leads to some inaccuracy due to averaging the ascending and descending passes.

A derived Sq from the DMSP SSM would only be good when investigating a magnetic storm with the same spacecraft magnetometer data. There are inherent differences in the instrument related error factors which were listed in section 2.7. The error factors listed are SSM calibration, the spacecraft D/C magnetic field, solar cell magnetic field, and the satellite's attitude. All of these error factors would have a slight difference for each DMSP satellite. Also, prior to F-15 launch, the SSM was not placed on a five meter boom. There are also differences in the DMSP satellites orbits that make each spacecraft cross the magnetic equator at different times. Therefore, a different Sq signal would need to be derived for each DMSP satellite.

4.3 Future Work

As stated in Section 2.4.1.1, use of the annual means for the horizontal component of the geomagnetic field, H, defined for each observatory for the current year and the four preceding years delays the final index computation over a year. To be operationally useful, a real-time or quick-look Dst, which uses only the mean H from the four preceding years, needs to be created. Kyoto University does provide this service on their website, but AFWA would like to have its own in-house method. Ownership of their own Dst would remove the dependence of outside sources assuring uninterrupted input

into future models (i.e. the Magnetospheric Specification and Forecast Model (MSFM)) and help with assessing spacecraft anomalies. I compared my DMSP derived Dst to Kyoto's final ground-based Dst index. If time permitted, and with more recent SSM data from AFRL, I would have compared my method to the real-time index. This research should lay the groundwork to use the DMSP to provide a real-time index from its magnetometer data.

A stated limitation to my Dst method is that a different solar quiet signal must be derived from each DMSP satellite. A useful future project would be to gather the Sq signal from other DMSP satellites and compare them to the F-15 values. This would be especially valuable to the post F-14 spacecrafts that have the SSM mounted to the 5 meter boom. A comparison of Sq values from F-15 and, say, F-13 (with body mounted SSM) probably would not compare very well. To fully understand a comparison between solar quiet signals of different DMSP satellites, the F-15 Sq signal depicted in Figures 3.2 and 3.3 show periodic variations that require further study.

Referring to Figure 4.1, the time frame of my data (2000 to 2003) is at range of the solar cycle corresponding to solar maximum. A great follow-up to this research would be to continue with my Sq derivation to include a solar minimum period as well as the entire 11-year solar cycle. This would require that the F-15 satellite be in operation until about 2007. With this information one would only have to determine which part of the solar cycle you're on and use the corresponding Sq signal to subtract from a stormy period to gain a Dst index.

Finally, the graphs of Figures 3.4 through 3.16 mostly show the DMSP derived Dst representing a weaker storm than the observed ground-based index. One would

expect the opposite with the satellite located approximately 850 km closer to the ring current. As already stated, Dst measures magnetic field changes at the magnetic equator due to the storm-time ring current where these changes are in the plane parallel to the ground. Variations in the magnetic field are mostly along the DMSP's Y-axis but not perfectly aligned with the magnetic meridian. Therefore, using only Delta By in my methodology may not be complete in measuring the changes. To encompass the effect of the Z component, Delta Bz should be added to future calculations of a DMSP derived Dst index.

Bibliography

Citrone, P., Web-Based Graphical Products to Assess and Predict Space Weather Impacts on Military Systems, *FYI No. 51*, Air Force Weather Agency, 2002.

Della-Rose, Devin J. "An Investigation of Variable-Time Interval 'K-Like' Geomagnetic Indices," Ph.D. Dissertation, Utah State University, 1999.

Hamilton, D.C., et al., Ring Current Development During the Great Geomagnetic Storm of February 1986, *J. Geophysics Res.*, 93, 14343, 1988.

Hathaway, D.H., *The Sunspot Cycle*, NASA, Marshall Space Flight Center, Science Directorate, 2004.

Rich, F.J., Factors for Errors of the DMSP and SSM, Email correspondence, AFRL, Space Vehicles Directorate, 2004

Rich, F.J., Ring Current Depiction, Email correspondence, AFRL, Space Vehicles Directorate 2004

Rich, F. J., Users Guide for the Topside Ionospheric Plasma Monitor (SSIES, SSIES-2, and SSIES-3) on Spacecraft of the Defense Meteorological Satellite Program (DMSP), *Environmental Research Papers No. 1151*, AFRL, Space Vehicles Directorate, 1994.

Rostoker, G., Geomagnetic Indices, *Reviews of Geophysics and Space Physics*, Vol. 10, No. 4, pp. 935-950, 1972.

Russell, C. T. and R. L. McPherron, Semi-annual variation of geomagnetic activity, *J. Geophys. Res., 78*, 92, 1973.

Southwest Research Institute Online Glossary, The Dst Index, 2004

Southwest Research Institute Online Glossary, The Ring Current, 2004

Sugiura, M. and Toyohisa, K., On Dst Index, *IAGA Bulletin*, No. 40, 1986.

Tascione, T. F., *Introduction to the Space Environment*, Krieger Publishing Company, 1994.

Zieger, B. and K. Mursula, Annual variation in near-Earth solar wind speed: Evidence for persistent north-south asymmetry related to solar magnetic polarity, *Geophys. Res. Lett., 25*, 841-844, 1998.

REPORT DOCUMENTATION PAGE

Form Approved
OMB No. 074-0188

1. REPORT DATE *(DD-MM-YYYY)*	**2. REPORT TYPE**	**3. DATES COVERED** *(From – To)*
01-03-2005	**Master's Thesis**	Jun 2004 – Mar 2005

4. TITLE AND SUBTITLE

DEVELOPMENT OF A DEFENSE METEOROLOGICAL SATELLITE PROGRAM (DMSP) F-15 DISTURBANCE STORM-TIME (Dst) INDEX

5a. CONTRACT NUMBER

5b. GRANT NUMBER

5c. PROGRAM ELEMENT NUMBER

6. AUTHOR(S)

Bono, James, M., Captain, USAF

5d. PROJECT NUMBER

5e. TASK NUMBER

5f. WORK UNIT NUMBER

7. PERFORMING ORGANIZATION NAMES(S) AND ADDRESS(S)
Air Force Institute of Technology
Graduate School of Engineering and Management (AFIT/EN)
2950 Hobson Way
WPAFB OH 45433-7765

8. PERFORMING ORGANIZATION REPORT NUMBER

AFIT/GAP/ENP/05-02

9. SPONSORING/MONITORING AGENCY NAME(S) AND ADDRESS(ES)
Air Force Weather Agency
Office of Public Affairs
106 Peacekeeper Drive, Suite 2N3
Offutt Air Force Base, NE 68113-4039

10. SPONSOR/MONITOR'S ACRONYM(S)

11. SPONSOR/MONITOR'S REPORT NUMBER(S)

12. DISTRIBUTION/AVAILABILITY STATEMENT
APPROVED FOR PUBLIC RELEASE; DISTRIBUTION UNLIMITED.

13. SUPPLEMENTARY NOTES

14. ABSTRACT

As the Department of Defense's use of space and space assets increases, so does its need for timely and accurate predictions of space weather conditions. A good understanding of the data from satellites together with data from ground stations can help model and determine variations in the space environment. An accurate, real-time Disturbance storm-time (Dst) index would be a primary input into current and future space weather models.
The Dst index is a measure of geomagnetic activity used to assess the severity of magnetic storms. The index is based on the average value of the horizontal component of the Earth's magnetic field measured at four ground-based observatories. Use of the Dst as an index of storm strength is possible since the strength of the surface magnetic field at low latitudes is proportional to the energy content of the ring current, which increases during magnetic storms. Since ground-based magnetometers are not Air Force owned, development of a Dst index using the magnetometer from a DMSP satellite would remove the Air Force Weather Agency's reliance on outside Dst sources This research presents a method to create a Dst-like index using the magnetometer of the DMSP F-15 satellite. The solar quiet signal was determined for this magnetometer, and the resulting "Dst" index was compared against the official World Data Center Dst for several magnetic storms. Statistical analysis was accomplished using the paired *t*-test which shows good agreement between the DMSP derived Dst and ground-based index. In all of the storms analyzed, statistical results; mean, standard deviation, confidence intervals, etc., were always an order of magnitude smaller than the presented factors for error.

15. SUBJECT TERMS
Dst Index, DMSP, Magnetometer, Special Sensor Magnetometer

16. SECURITY CLASSIFICATION OF:			**17. LIMITATION OF ABSTRACT**	**18. NUMBER OF PAGES**	**19a. NAME OF RESPONSIBLE PERSON**
REPORT	**ABSTRACT**	**c. THIS PAGE**			Devin Della-Rose, Maj, USAF (ENP)
U	**U**	**U**	**UU**	78	**19b. TELEPHONE NUMBER** *(Include area code)* (937) 255-3636, ext 4514; e-mail: Devin.DellaRose@afit.edu

Standard Form 298 (Rev: 8-98)
Prescribed by ANSI Std. Z39-18